EFFECT OF AXIAL LOADING ON THE LATERAL BEHAVIOUR OF THE PRECAST POST-TENSIONED SEGMENTAL COLUMN

MUHAMAD ARIF BIN AHMAD

CIVIL AND ENVIRONMENTAL ENGINEERING

UNIVERSITI TEKNOLOGI PETRONAS

SEPTEMBER 2016

Effect of Axial Loading On the Lateral Behaviour of the Precast Post-Tensioned Segmental Column

by

Muhamad Arif Bin Ahmad

17119

Dissertation submitted in partial fulfilment of
the requirements for the
Bachelor of Engineering (Hons)
(Civil and Environmental Engineering)

SEPTEMBER 2016

Universiti Teknologi PETRONAS,
32610, Bandar Seri Iskandar,
Perak Darul Ridzuan

CERTIFICATION OF APPROVAL

Effect of Axial Loading On the Lateral Behaviour of the Precast Post-Tensioned Segmental Column

by

Muhamad Arif Bin Ahmad

17119

A project dissertation submitted to the
Civil and Environmental Engineering Programme
Universiti Teknologi PETRONAS
in partial fulfilment of the requirement for the
BACHELOR OF ENGINEERING (Hons)
(CIVIL AND ENVIRONMENTAL ENGINEERING)

Approved by,

_____

(Dr. Ehsan Hasan Nikbakht)

UNIVERSITI TEKNOLOGI PETRONAS
BANDAR SERI ISKANDAR, PERAK
September 2016

CERTIFICATION OF ORIGINALITY

This is to certify that I am responsible for the work submitted in this project, that the original work is my own except as specified in the references and acknowledgements, and that the original work contained herein have not been undertaken or done by unspecified sources or persons.

_____

MUHAMAD ARIF BIN AHMAD

ABSTRACT

Precast post-tensioned segmental columns were on the rise to satisfy the construction needs for the past years especially in bridge construction and in region with high seismic activity. The construction speed was reported to have been accelerated by 50% when precast. The purpose of this project is to study the effect of axial loading on lateral behaviour of precast post-tensioned segmental columns by modelling a 3D non-linear finite element model of the columns. The precast post-tensioned segmental column used in this project adopts the hybrid system that fully utilised the combination between mild steel reinforcement and post-tensioned tendon. This combination enables the segmental column to exhibit self-centring capability from the elastic reaction of the unbonded post-tensioned tendons and better energy dissipation from mild steel reinforcement to achieve hysteretic response. This project was broken down into three stages. Stage 1 is the development stage of initial modelling of non-linear finite element column models in ANSYS for validation with existing experimental results before any further development is made on the model. Stage 2 is the stage where parametric studies of the modelling started. A set of parameters includes initial post-tensioning force, axial loading, number of column segments, and concrete strength were used. At Stage 3, the results were analysed with regard to each parameter studied and the effect of axial loading in each cases are emphasized. From the results obtained, it can be seen that axial loading plays an important role for the column rigidity. The outcome from this project may help to give an understanding on affected lateral behaviour of the precast post-tensioned segmental column when axial loading is applied.

ACKNOWLEDGEMENT

I want to express my appreciation and thanks to my supervisor, Dr. Ehsan Nikbakht, for his time to guide during the modelling process which make this research possible. I would like to thank my friends that stay with me throughout this research and for their immense support.

TABLE OF CONTENTS

LIST OF FIGURES

LIST OF TABLES

CHAPTER 1

INTRODUCTION

1.1 Background of Study

Precast segmental bridge columns have gained increasing attention from researchers worldwide. According to Transportation Research Board (TRB) (2003), precast structural elements offers the advantages of reducing the on-site construction time where it can be fabricated off-site and assembled in relatively short time hence remove the necessity for closing the access road during construction while construction quality is maintained and reduced life-cycle cost and environmental impact. In using precast structural elements, the construction progress increased by 50% as concluded from a study by Shahawy (2003) sponsored by the US Texas Department of Transportation (TxDOT) and the Federal Highway Administration (FHWA).

This project focus is on the precast hybrid post-tensioned segmental bridge columns. Precast post-tensioned segmental bridge column is a column structure where each segments are stacked onto one another which then connected structurally together by a continuous post-tensioning tendons anchored on the column foundation footing and column top. In hybrid systems, the post-tensioning tendons are coupled with mild steel reinforcements to achieve self-centring capability and good energy dissipation capacity. This column structure arrangement can be used to predict the pushover lateral force-displacement of segmental columns as proposed by Hewes and Priestley (2002).

In this project, the precast post-tensioned segmental columns will be subjected to horizontal lateral load and imposed by vertical axial load acting as the gravity load on the column structure to study the lateral displacement of column and damages occur at the base of the column affected by the axial loading applied.

1.2 Problem Statement

The construction of conventional monolithic bridge columns imposed limitations where the constructions have to be done on-site that it is very time consuming and the cut off of the access roads for the work zone safety. By substituting the conventional monolithic bridge columns with precast post-tensioned segmental columns, each and every component can be constructed off-site including the segments and column footing and assembled in a short time without the closing of the access roads. The precast post-tensioned segmental columns are fabricated simultaneously per segments in the controlled environment where the quality is ensured.

The conventional monolithic bridge columns show a ductile behaviour when subjected to lateral loading which then suffer from formation of plastic hinges that produces crack and damages at critical area (base of column), leads to an expensive cost for repairs. By using the precast post-tensioned segmental columns, the segments joints allow for the lateral displacement of column structure due to effect of lateral loading where the formation of plastic hinges are eliminated with the implementation of discontinuous mild steel reinforcement through column segments joints and self-centring capability from the unbonded post-tensioning tendons through the duct at the centre of precast column segments.

1.3 Objectives of Study

The objectives of this study are as following:

1. To investigate the effect of axial loading on lateral behaviour of the precast post-tensioned segmental columns.
2. To conduct a parametric study on the 3D non-linear finite element model of the precast post-tensioned segmental column such as initial post-tensioning force, axial loading, number of segments in ANSYS, and concrete strength.

1.4 Scope of Study

This project focuses on the investigation of the effect of axial loading on the lateral behaviour of the precast post-tensioned segmental columns in which pushover lateral force-displacement is concerned. This project will be broken down into three stages. Stage 1 will be the development of initial modelling of non-linear finite element model in ANSYS for validation with existing experimental results before any further development is made on the model. Stage 2 will be the start of parametric study of the modelling where a set of parameters for initial post-tensioning force, axial loading and concrete strength are introduced. The results obtained from parametric studies of each set of parameters will then enter final stage, where analysis on the axial loading effects on the lateral behaviour of the precast post-tensioned segmental column is made.

CHAPTER 2

LITERATURE REVIEW

2.1 Introduction

Precast concrete is a structural system that consists of plant-fabricated columns, shear walls, beams and double tees; make up the floor system, which is transported and erected on-site. Recently, the attention and usage of precast segmental structure have increased due to its reduction in construction time and cost, and the efficiency in reducing the environmental impact while improving construction quality. According to Transportation Research Board (TRB) (2003), precast structural elements offers the advantages of reducing the on-site construction time where it can be fabricated off-site and assembled in relatively short time hence remove the necessity for closing the access road during construction while construction quality is maintained and reduced life-cycle cost and environmental impact.

This project's aim is to investigate the effect of axial loading on the lateral behaviour of precast post-tensioned segmental columns. The definition and concepts are discussed in sections hereafter.

2.2 Precast Post-Tensioned Segmental Columns

Precast post-tensioned segmental columns are a column structure where each segments are stacked onto one another which then connected structurally together by a continuous post-tensioning tendons anchored on the column foundation footing and column top as shown in Figure 2.1 (b) and (c). Figure 2.1 (a) shows the monolithic reinforced concrete column. All three columns in Figure 2.1 have steel plates layered on top of the column

top as added mass to substitute axial loading, resulting in no additional axial loading applied (Zhang et al., 2016). The continuous post-tensioning tendons can be used in two methods; bonded and unbonded. In bonded post-tensioning method, the corrugated hollow steel ducts are grouted with cementitious materials after the stressing of tendons that will result in the full interaction (bond) between the tendons and surrounding concrete. In unbonded post-tensioning method, the tendons are placed through the hollow duct in the column segments as to reduce or avoid the possibility of tendons yielding under strong lateral loading, resulting in self-centring capability with the preserved clamping force needed to hold the column segments together. Studies on bonded post-tensioning can be found in Shim et al. (2008) and Kim et al. (2010), while studies on unbonded post-tensioning can be found in Hewes and Priestley (2002), Ou et al. (2007), Dawood et al. (2012), Chou et al. (2013), Hari et al. (2014) and, Zhang et al. (2016).

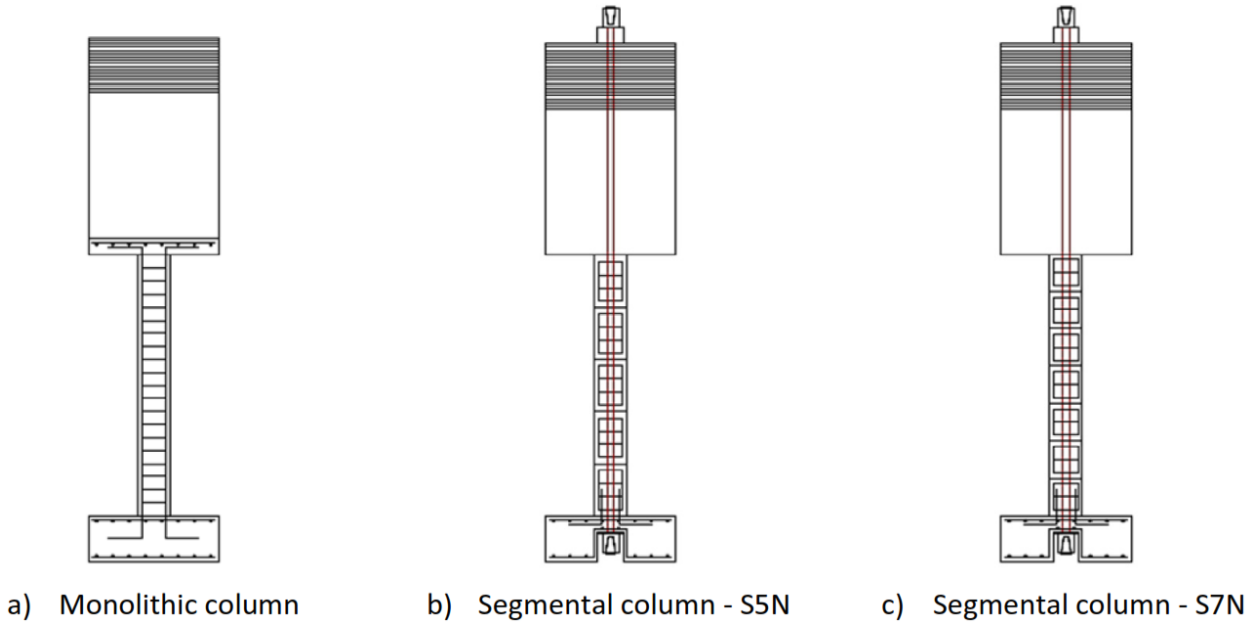

Figure 2.1: Schematic views of column specimens. (Zhang et al., 2016)

The behaviour of precast post-tensioned segmental columns differs fundamentally from that of monolithic reinforced concrete columns when subjected to seismic loading, in which the response similar to a rocking mechanism, where the column segments opened when the moment resistance provided by the post-tensioning tendons is overcome. Figure

2.2 shows the column deformation in stages, at stage 3, the right side of segment 1 and 2 of the column undergo concrete crushing from the compression due to pushover lateral deformation and the appearances of segments opening. The column segments opening prevent the formation of plastic hinge (concrete crack in tension and crushed in compression) at hinge area at column base. According to Kim et al. (2010), the rigid rotation of the column in entirety at column base in precast segmental bridge column contributed to most structural deformation and not due to plastic deformation at hinge area. Kim et al. (2010) reported that no shear failure such shear slip at segmental joints or concrete shear failure within segments was found.

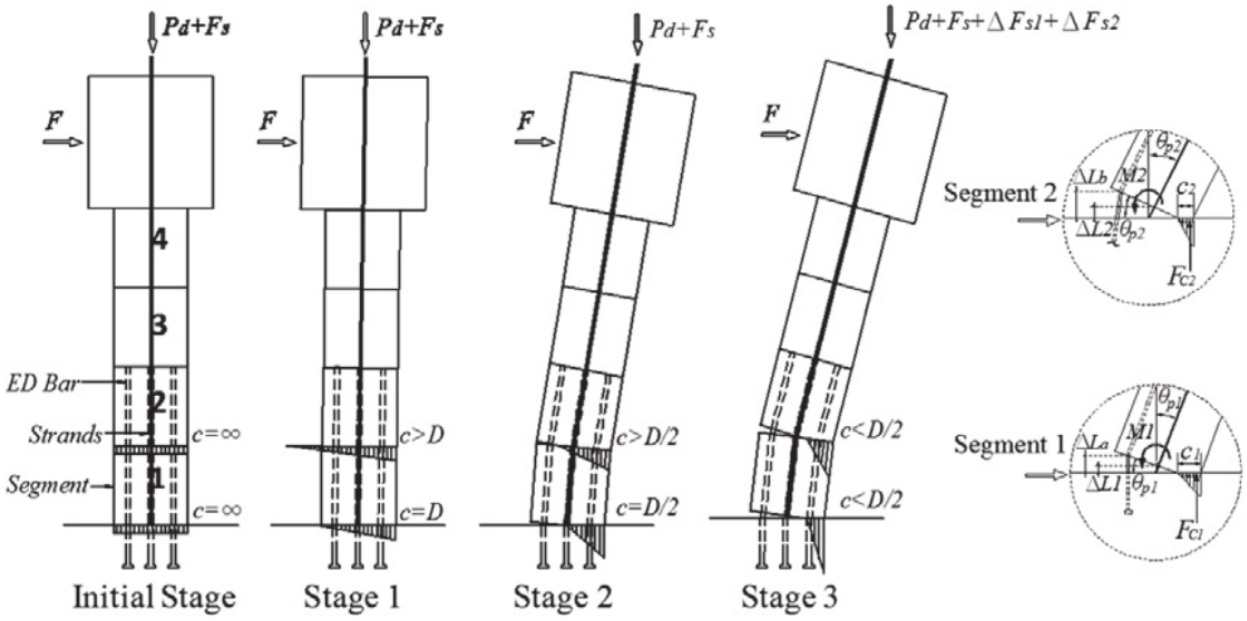

Figure 2.2: Column deformation under lateral loading. (Chou et al., 2013)

2.3 Hybrid System

The precast post-tensioned segmental column in this project adopted the hybrid system introduced by Stone et al. (1995), where its primary use was for beam-column connections. According to Ou et al. (2007), precast hybrid system can be summarised as a system with

proper combination between the post-tensioning tendons and the mild steel reinforcements across the precast joints with the objective to produce satisfactory hysteretic energy dissipation and small residual displacement upon unloading from the flag-shape hysteretic behaviour. Figure 2.3 (c) shows the hysteretic response of hybrid system.

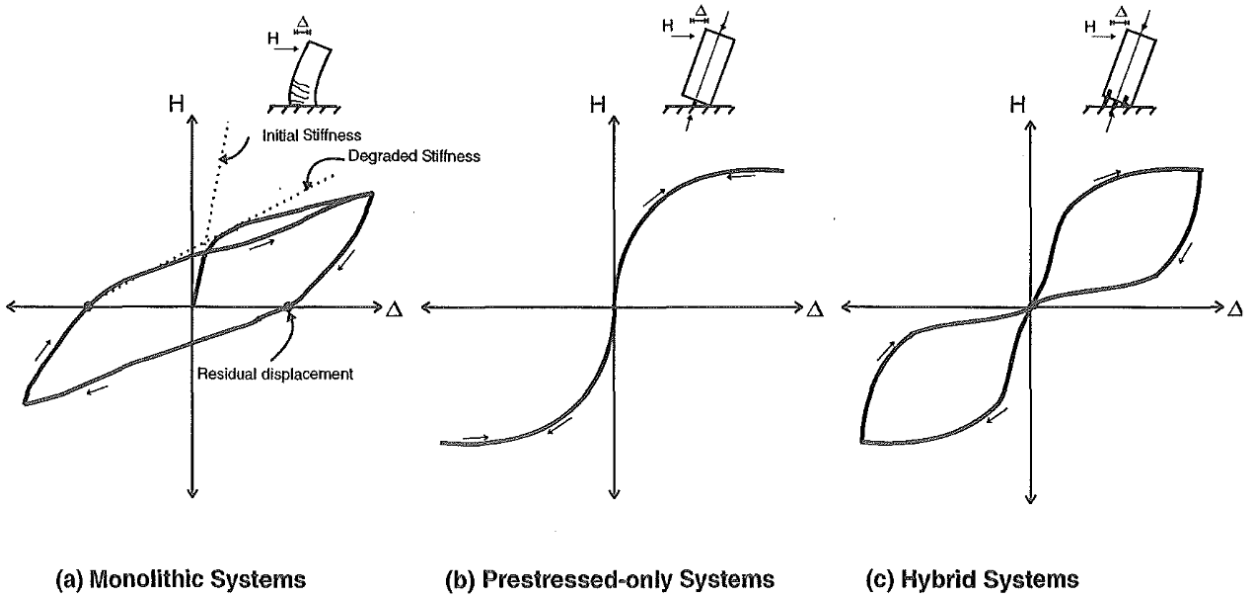

Figure 2.3: Hysteretic response of various structural system. (Holden, 2001)

The post-tensioning tendons in hybrid system are left unbonded to maintain the elasticity when subjected to lateral loading, resulting in self-centring capability. The initial stress from the post-tensioning tendons acts as a primary lateral force resistance for the column. Self-centring in precast post-tensioned segmental columns means that the columns will return to its original position before loading is applied. The presence of mild steel reinforcements bars is to acts as energy dissipater for the precast segmental column structure.

CHAPTER 3

METHODOLOGY

3.1 Research Methodology

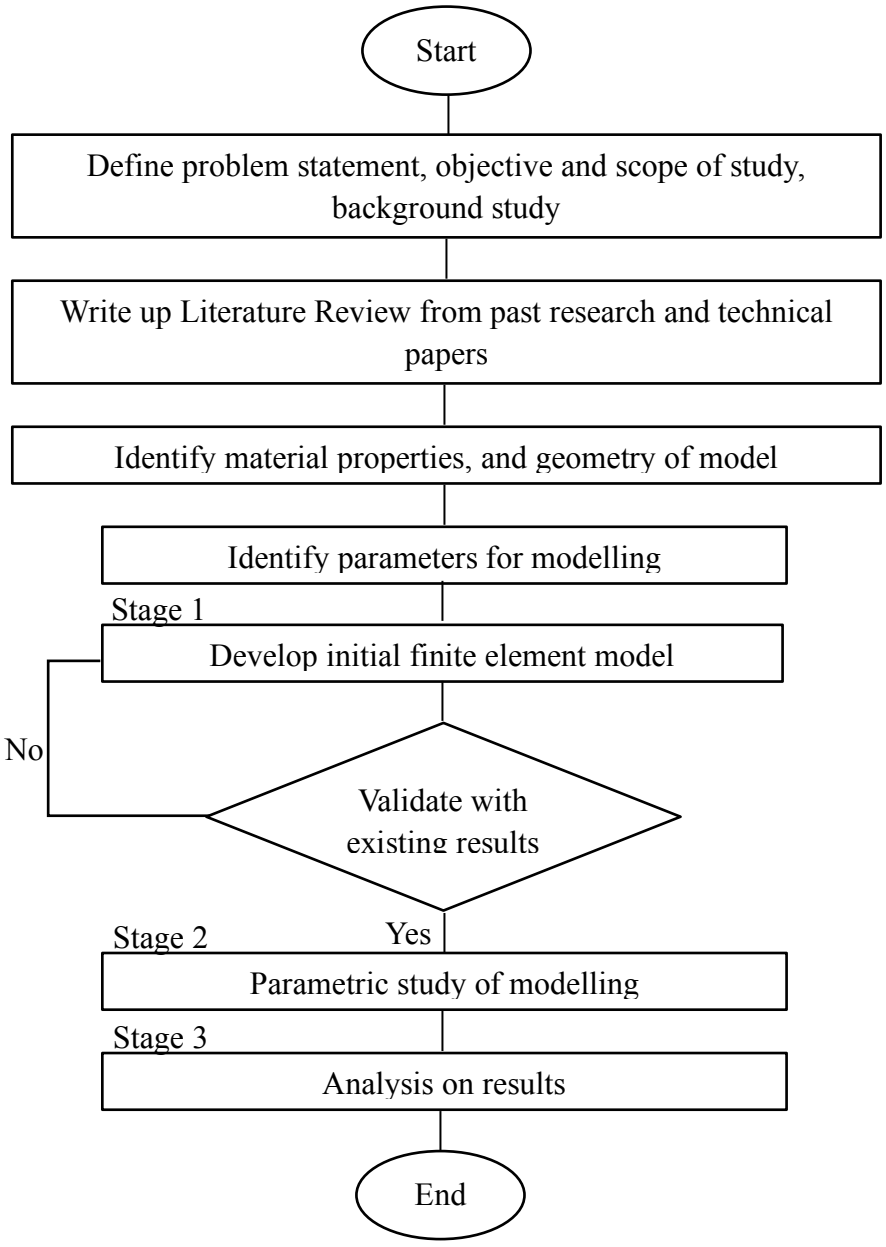

Figure 3.1: Project Flow Chart.

3.2 Finite Element Method (FEM)

The non-linear finite element model of the precast post-tensioned segmental column will be developed to investigate the behaviour of the column against the lateral loading under the imposition of axial loading. For this, the software ANSYS 15 (2015) will be used. The results obtained will then be compared and validated with existing experimental result.

3.2.1 Stress-strain Curve of Concrete

Figure 3.2 shows the typical stress-strain curve for normal weight concrete developed by Bangash (1989).

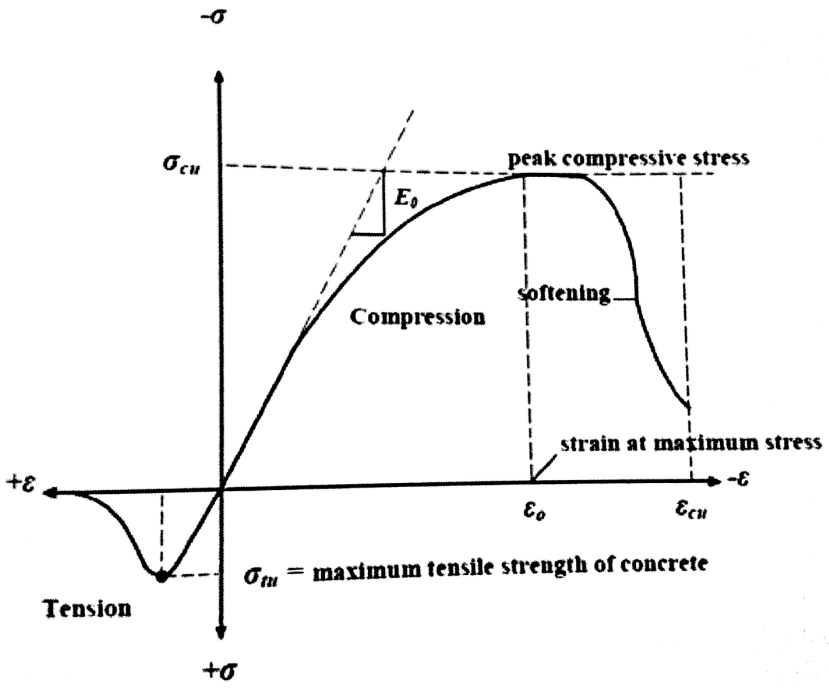

Figure 3.2: Typical biaxial compressive and tensile stress-strain curve for concrete. (Bangash, 1989)

Where E_o is defined as modulus of elasticity of concrete; σ_{cu} is defined as peak compressive stress; σ_{tu} is defined as maximum tensile strength of concrete; ε_{cu} is defined as peak compressive strain; and ε_o is defined as strain at the maximum stress. The ultimate concrete compressive and tensile stress for concrete column segment was calculated as:

$$\sigma_{cu} = \left(\frac{E_o}{4700}\right)^2$$

$$\sigma_{tu} = 0.62\sqrt{\sigma_{cu}}$$

σ_{cu} and σ_{tu} are in MPa

3.2.2 Stress-strain Model for Prestressing Steel

The curve shown in Figure 3.3 are constructed from the following equations.

Prestress steel limit of proportionality: $\varepsilon_{lp} = 0.0086$

Reduced ultimate prestress steel strain: $\varepsilon_{lp} = 0.0300$

$$\varepsilon_s \leq 0.0086: f_s = 28500\varepsilon_s$$

$$\varepsilon_s \leq 0.0086: f_s = 270 - \frac{0.04}{\varepsilon_s - 0.007}$$

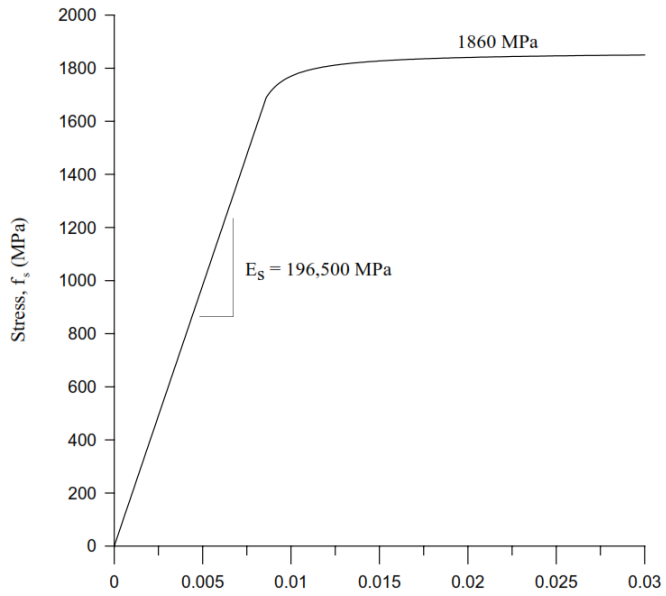

Figure 3.3: Prestressing steel stress-strain model. (Hewes and Priestley, 2002)

3.2.3 Material Properties, Models Geometry and Parametric Study parameters

Table below shows the material properties and geometry used by Hewes and Priestley (2002) for their test specimens. The tabulated properties below are used in initial column model as well as in other parametric models, except for concrete grade that will have variance in parametric study.

Table 3.1: Material properties.

Material	Grade	Elasticity (MPa)	Strength (MPa)
Concrete	40	29260	$f_c = 41.4$ $f_t = 4.053$
Reinforcement	-	200000	$f_y = 410.0$
Prestressing Steel	-	200000	$f_{py} = 1800$

Table 3.2: Geometry of models.

Components	Dimension (mm)	Quantity	Thickness (mm)
Post-tensioning Strands	12.7 diameter	1	-
Longitudinal Reinforcement	12.7 diameter	8	-
Central Duct	140	-	-
Column	610 diameters	-	-
Column Head	950 x 950	-	-
Column Footing	1400 x 1400	-	-

Table 3.3: Parametric values for parametric study of the column modelling.

Element	Parameter	No. of models
Initial Prestressing	20% - 80%	24
Axial Loading	400 kN – 2400 kN	11
Column Segments	3 and 5 segments	2
Concrete Strength	G30, G50, and G75	12

Total number of column models developed are 50 that include one initial model. The column model is developed based on the dimensions shown in Figure 3.4 in half-section and the symmetry boundary condition is applied to the cross-section of the column model.

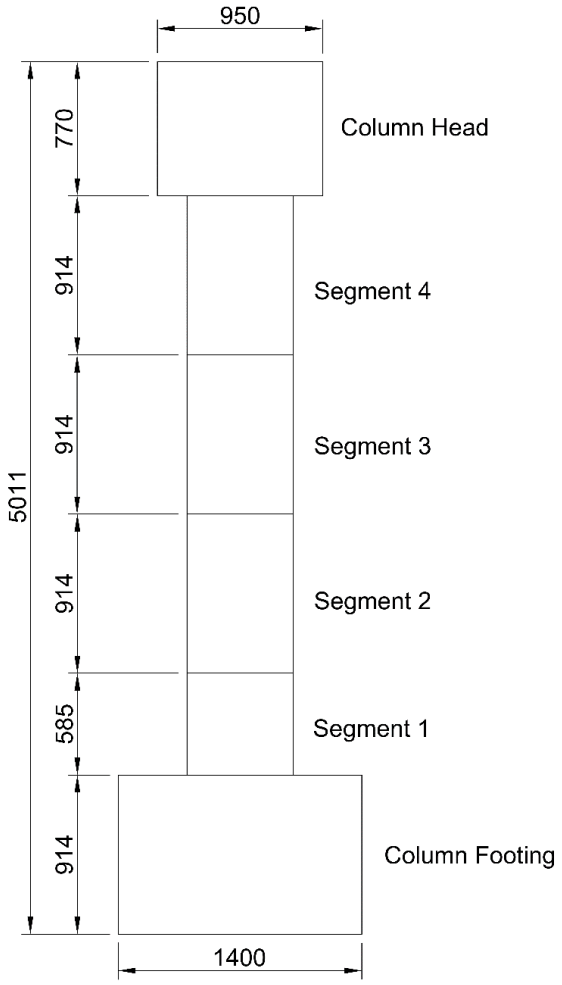

Figure 3.4: Column dimension for modelling.

3.2.4 Modelling of Segmental Columns

In this section, the modelling procedure of the precast segmental column will be presented.

1. Open ANSY Mechanical APDL 15. The interface will be as shown in Figure 3.5.

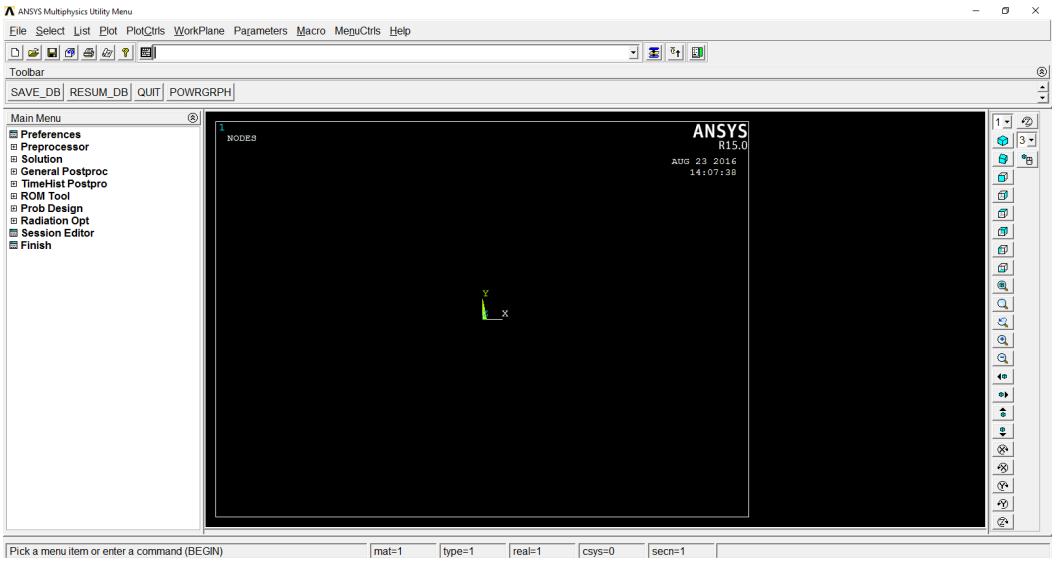

Figure 3.5: ANSYS Mechanical APDL 15 interface.

2. Change the preferences to structural as shown in Figure 3.6.

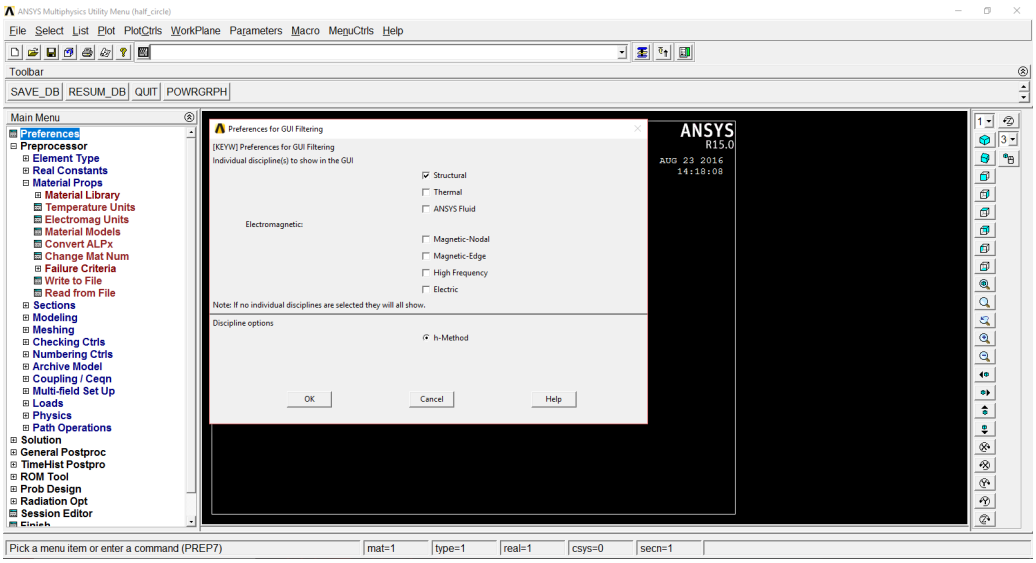

Figure 3.6: Preferences for Graphical User Interface (GUI) filtering.

3. In the main menu, go to Preprocessor > Element Type > Add/Edit/Delete to define the element to be used for the model as shown in Figure 3.7. The list of types of element will be in next section.

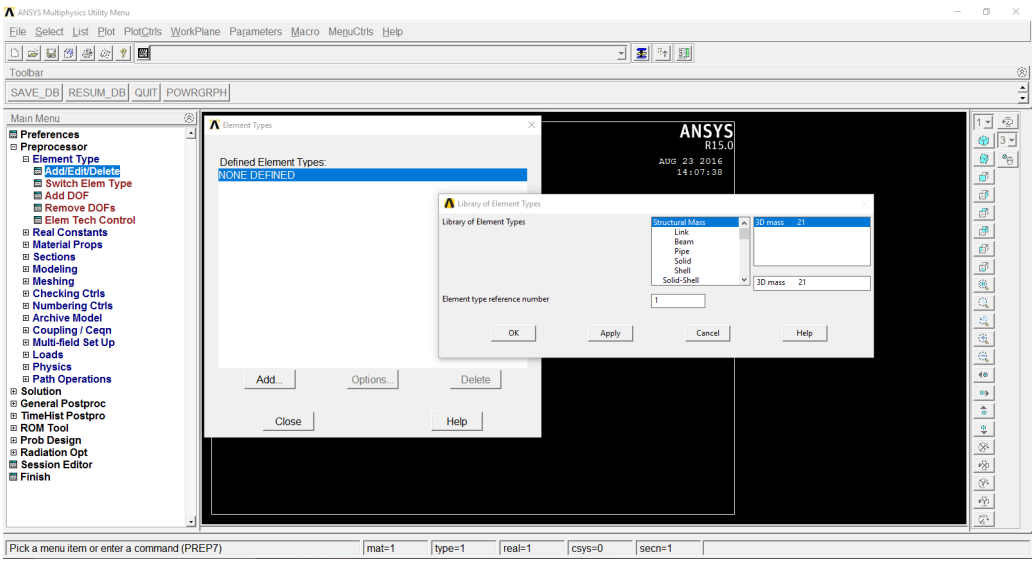

Figure 3.7: Defining element types for the model.

4. In the main menu, go to Preprocessor > Real Constants > Add/Edit/Delete to define the real constant for the defined element types as shown in Figure 3.8. Figure 3.9 shows the windows for the real constants of Solid65.

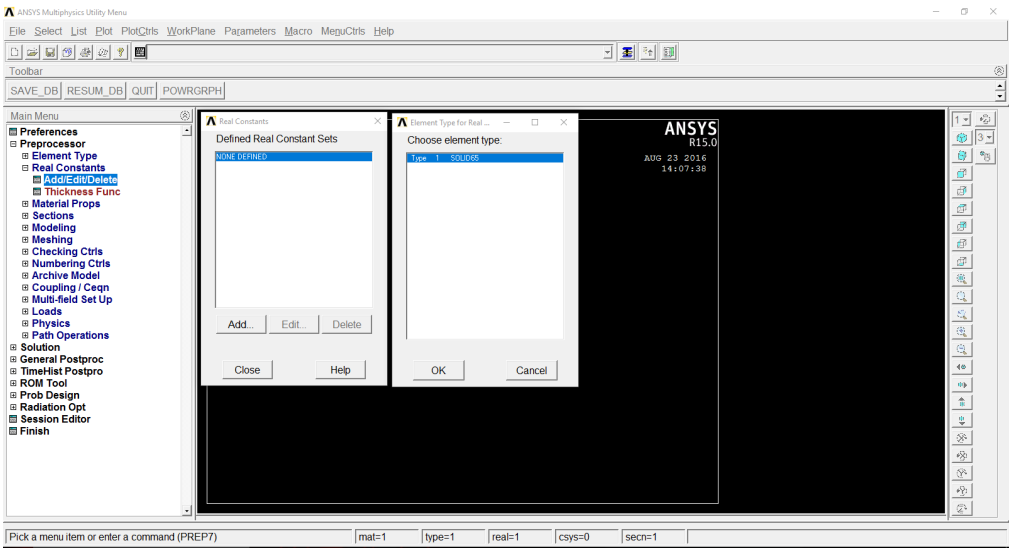

Figure 3.8: Defining real constants for each element types.

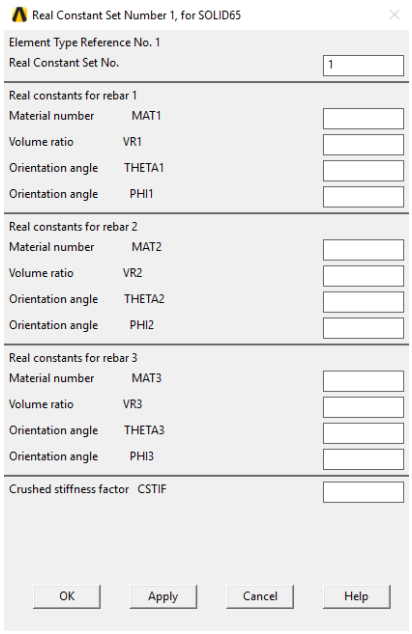

Figure 3.9: Real constants for Solid65.

5. In the main menu, go to Preprocessor > Material Models to define properties of the material as shown in Figure 3.10, Figure 3.11, and Figure 3.13. The graph obtained from the values for stress-strain in Figure 3.11 is shown in Figure 3.12. The following figures show the material properties of concrete.

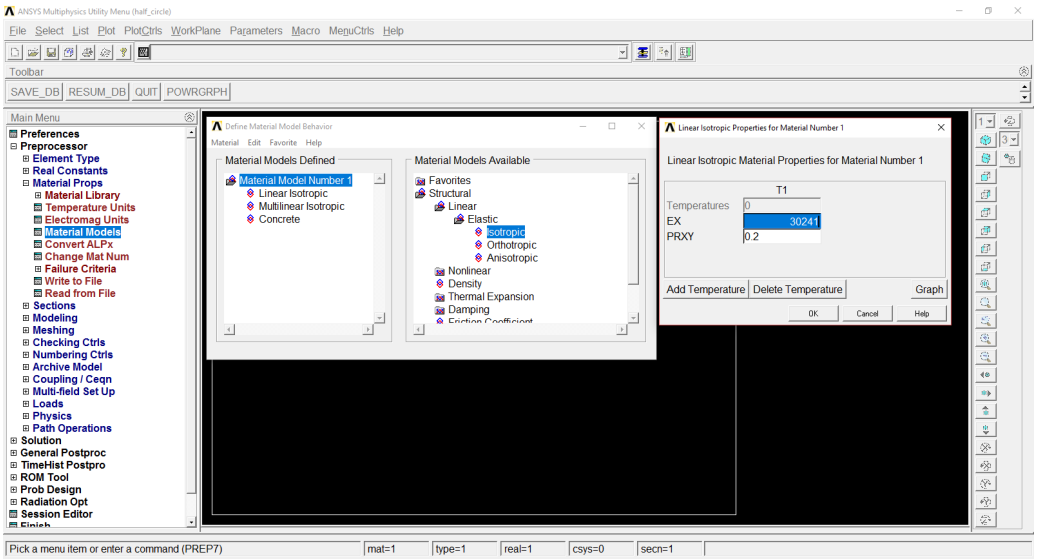

Figure 3.10: Elastic properties of concrete.

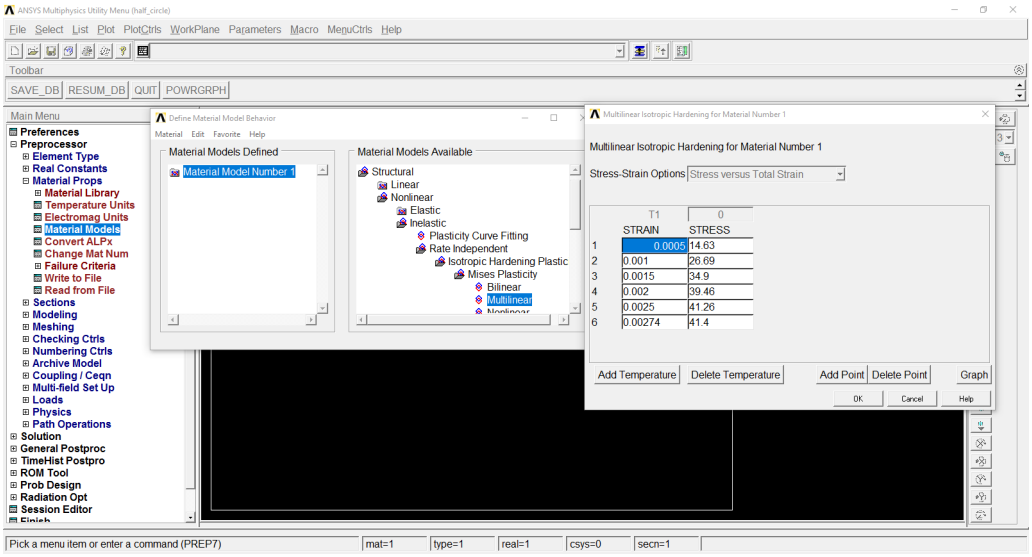

Figure 3.11: Stress-Strain values for G40 concrete.

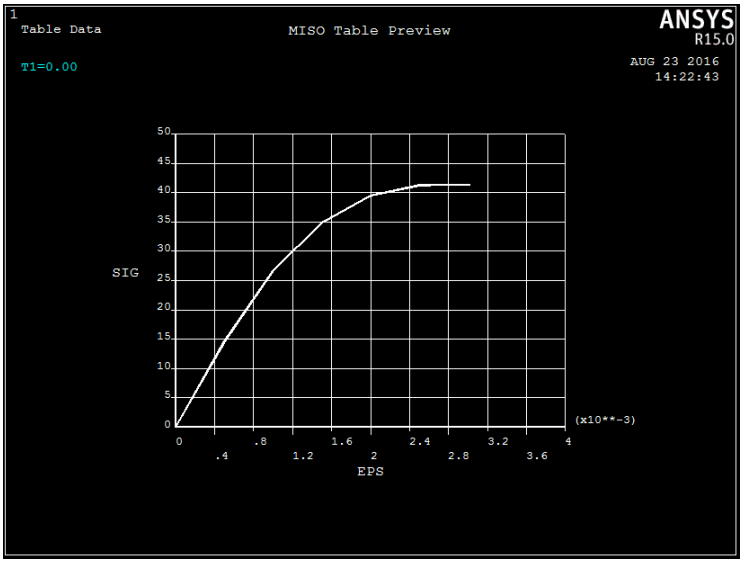

Figure 3.12: Stress-Strain graph of concrete from input values.

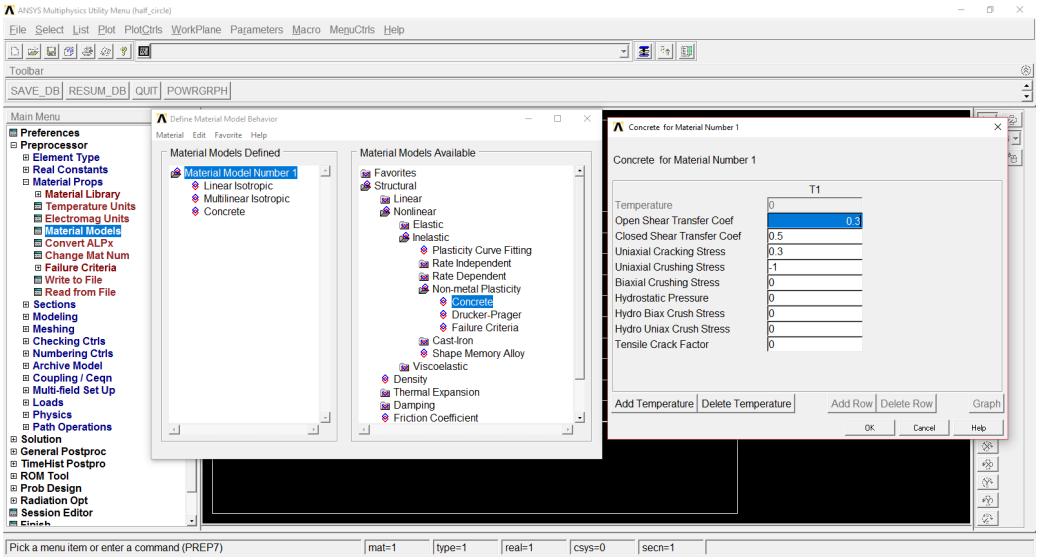

Figure 3.13: Non-metal plasticity properties of concrete.

6. Change the active Coordinate System (CS) to Global Cylindrical Y by going to Workplane > Change Active CS to > Global Cylindrical Y as shown in Figure 3.14. This will make the Y-axis the central axis for circular-shaped model.

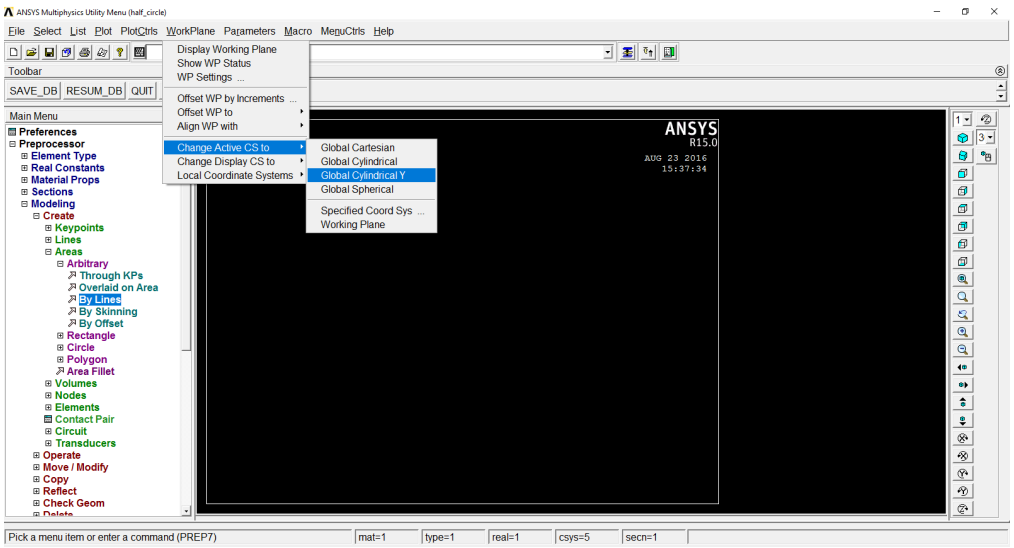

Figure 3.14: Changing of Workplane system.

7. Now, the modelling can start. In the main menu, go to Preprocessor > Modelling > Create > Keypoints > In Active CS as shown in Figure 3.15. The X-axis will be the diameter of the circle, and Y-axis as the angle in degree. Z-axis will be 0.

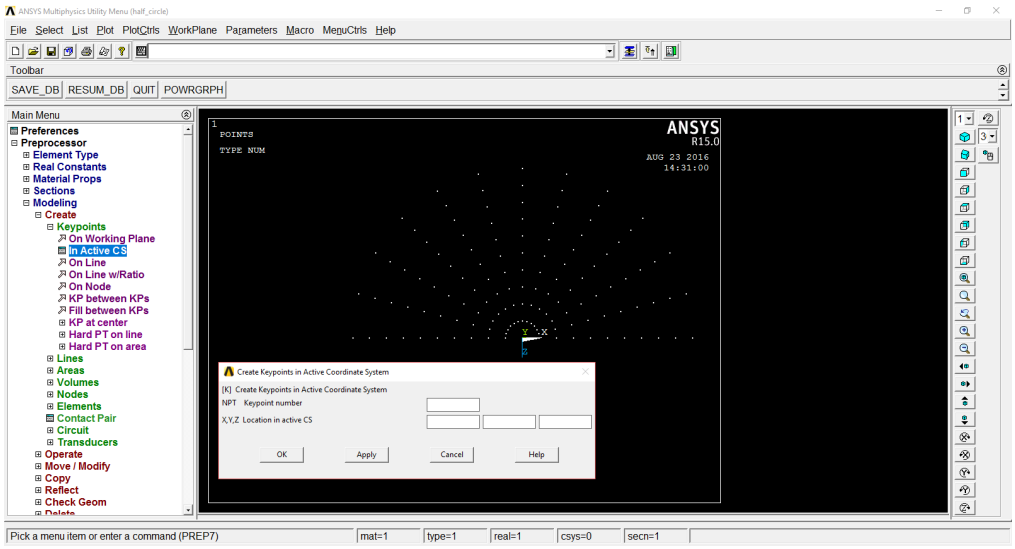

Figure 3.15: Creating Keypoints.

8. In the main menu, go to Preprocessor > Modelling > Create > Lines > In Active Coord as shown in Figure 3.16. The arc will be automatically formed as keypoints being connected in circular manner.

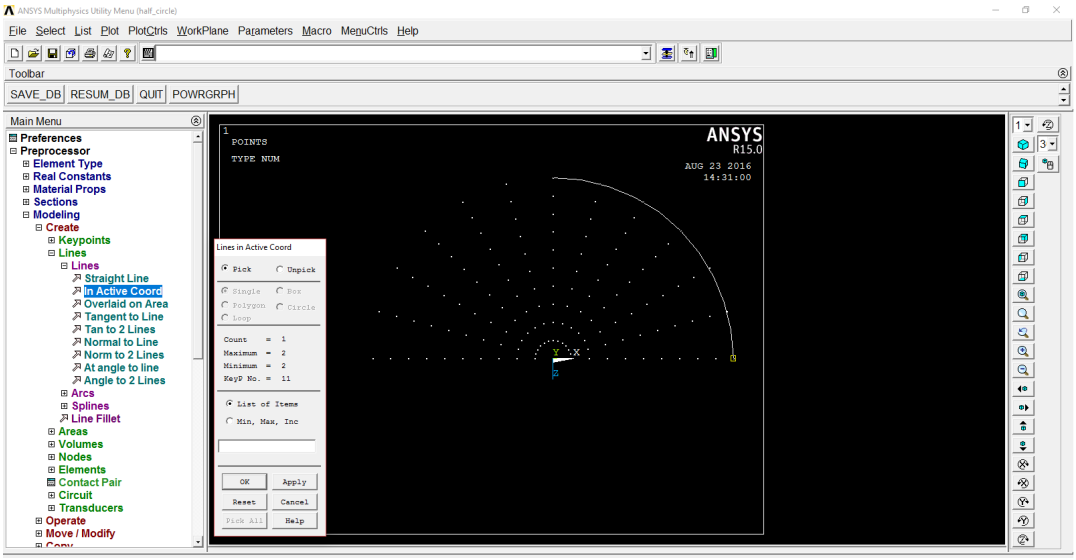

Figure 3.16: Creating lines from keypoints.

9. In the main menu, go to Preprocessor > Modelling > Create > Area > Arbitrary > By Lines as shown in Figure 3.17. The area to be create must be enclosed by connected lines, else it will return an error message.

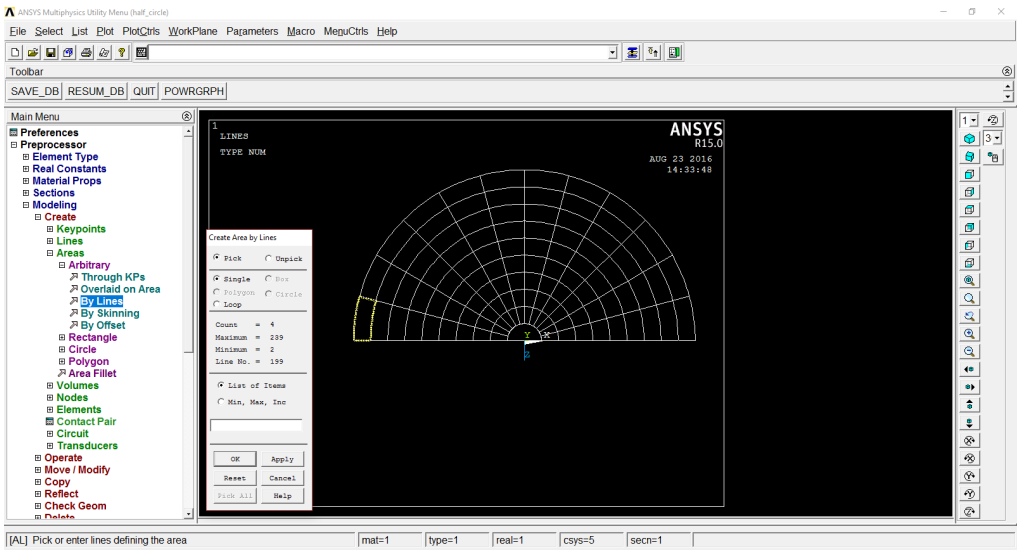

Figure 3.17: Creating an area from enclosed lines.

10. In the main menu, go to Preprocessor > Modelling > Operate > Extrude > Areas > By XYZ Offset as shown in Figure 3.18. Input the preferred extrusion values. This will create the volume for the model.

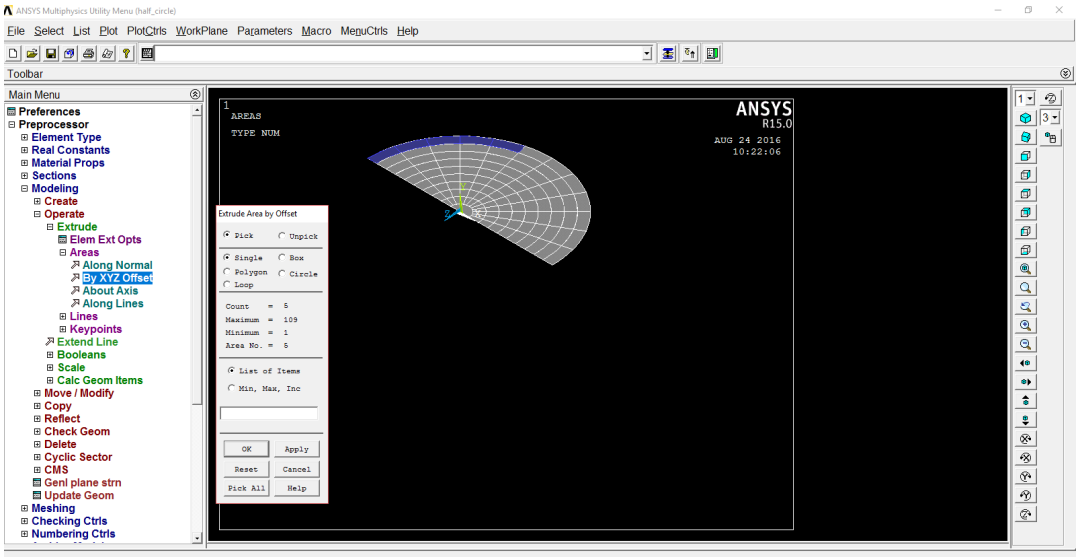

Figure 3.18: Extrusion of area for column segment.

11. On the menu, go to Select > Everything to select the model, the go to Select > Entities. A window will show up and from the first dropdown menu and second dropdown menu, choose Area and By Location as shown in Figure 3.19. Input the preferred location (use the last extruded value).

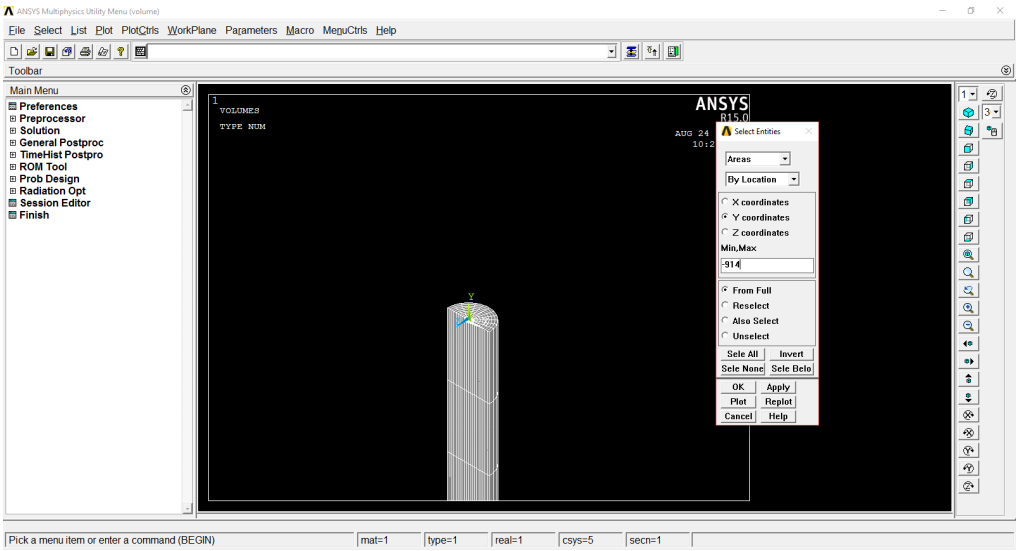

Figure 3.19: Selecting entities like area to a preferred location.

12. In the main menu, go to Preprocessor > Modelling > Copy > Areas to copy the surface area of the column. Repeat Step 10 for the extrusion of the area. The copied area will emulate the contact friction with the use of contact and target element.
13. Repeat Step 11 to 12 to create the segmental columns. The column segments are shown in Figure 3.20.
14. To create the column footing and column head:
    a. Repeat Step 11.
    b. Repeat Step 7 to 10 to create keypoints, then lines and lastly area of the column footing and column head. Then extrude to get its volume.
15. The full model is as shown in Figure 3.21.

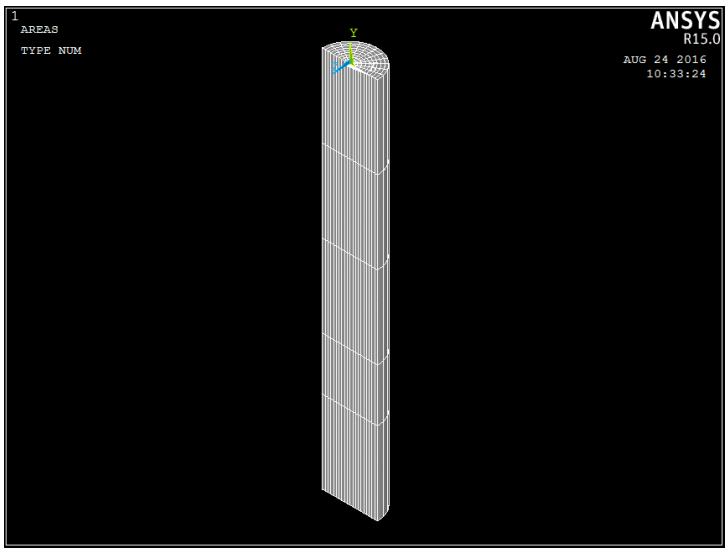

Figure 3.20: Model of column segment.

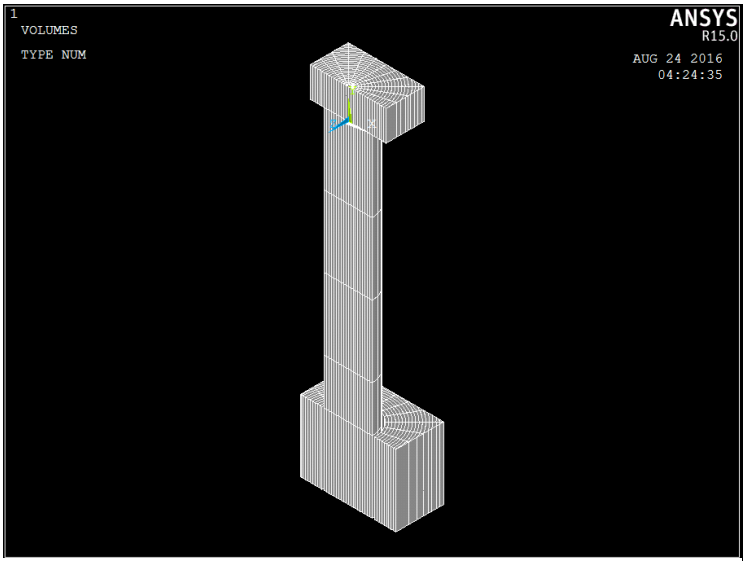

Figure 3.21: Full model of the columns.

From the modelling of the segmental columns, it will undergo simulation to obtained the results that will be compared and validated before parametric study of the modelling begin. ANSYS Mechanical APDL 15 will be used for the purpose of modelling and running the simulation. It crucial to first identify the types of element to model in ANSYS and proper loading procedure before modelling work started.

3.2.5 Types of Elements

In ANSYS, there are elements that can be used to represent or model the precast post-tensioned segmental columns. Below is the list of elements can be used:

1. Solid65 for modelling the concrete element of the column.
2. Link8 is used for post-tensioning tendons element.
3. Solid185 for the mild steel reinforcement element.
4. Contact and Target element for the contact surface for each column segment joints.

For Link8, a bit of command programming is needed to enable the element to be used in ANSYS 15.

ET, 30, LINK8 (element type, element number, element category)

R, 30, 1332, 0.00041 [real constant, ID number (should be same with element number, real constant 1 (area), real constant 2(initial strain)]

The above commands are written in ANSYS Mechanical APDL to enable the use of LINK8 element that is recently not supported in the ANSYS 15. The functionality of the LINK8 remains the same as in previous versions of ANSYS.

3.2.7 Loading Procedure

Three types of loading are imposed at three stages as outlined below: post-tensioning pretension, axial loading and pushover lateral loading. The footing is assumed fixed at the bottom in all stages.

1. Applying initial prestressing of post-tensioning tendons of 82 MPa (0.00041 strain) equivalent to 4.5% of the 1800 MPa tensile strength. As for parametric studies, the initial prestressing are applied with range from minimum 20% to maximum 80% of the tensile strength. The initial prestressing values are calculated from equation: $\sigma = E\varepsilon$ (where σ is the initial prestressing, E is the Elastic Modulus, and ε is the post-tensioning tendon strain). The tendon's strain value is the input value for the initial strain in the ANSYS command programming.

2. Applying an axial loading that acts as gravity load of 846.93 kN initially. As for parametric studies, the axial loading values ranging from minimum 400 kN to maximum 2400 kN with increment of 200 kN for each models. The axial loading values are calculated from equation: $0.07F'_cA_c$ (where F'_c is the compressive strength of concrete and A_c is the cross-sectional area of cylindrical column segments)
3. Applying a lateral loading at the head of the column, increased until the crushing at the column base occur. The lateral loading applied are in the form of lateral displacement where the lateral force data will be acquired after the simulation is done. In this project, the lateral displacement applied is 150 mm.

CHAPTER 4

RESULTS AND DISCUSSION

4.1 Numerical Results Comparison

4.1.1 Initial Prestressing Parameter

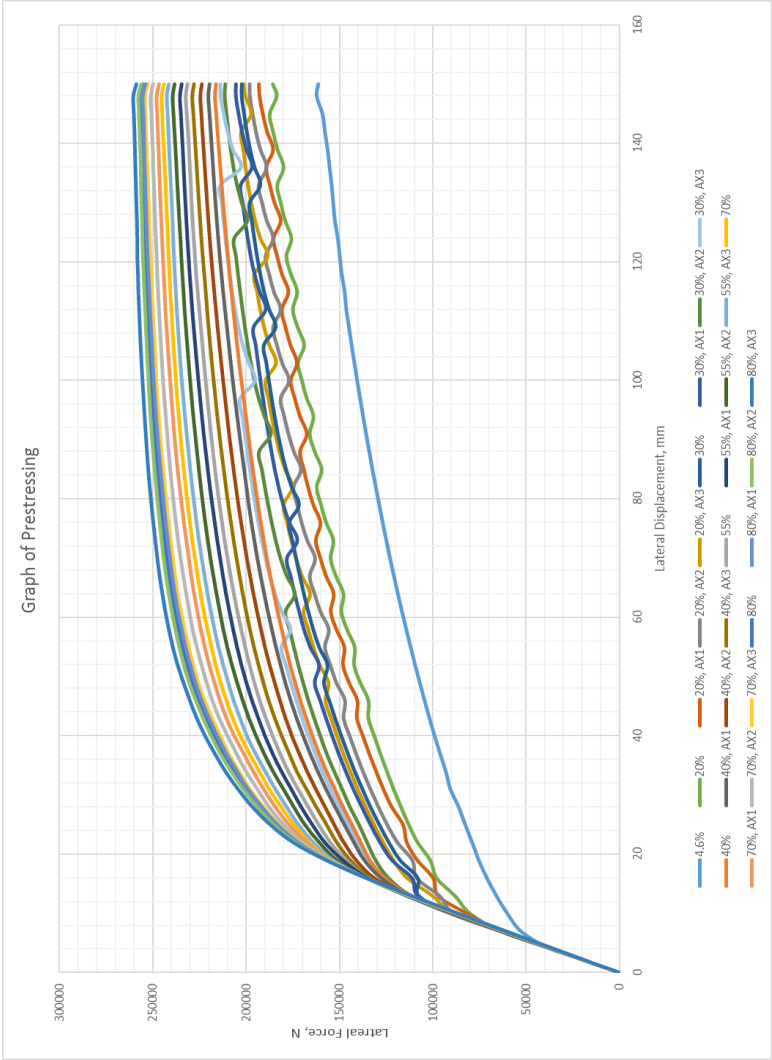

Figure 4.1: Graph of initial prestressing of post-tensioning tendons.

Figure 4.1 shows the comparison of all 25 results for initial prestressing conditions. The initial prestressing conditions applied are 4.6%, 20%, 30%, 40%, 55%, 70% and 80% with each conditions have addition of three axial loading conditions applied of 1000 kN, 1200 kN, and 1400 kN labelled as AX1, AX2 and AX3 respectively with an exception to the preliminary condition of 4.6%. The results acquired are taken from the precast segmental post-tensioned column undergone 150 mm lateral displacement simulation. The preliminary result implement 4.5% (82 MPa) for the initial prestressing resulting in 162 kN of lateral loading. The result from parametric study on initial prestressing for 20%, 20%:AX1, 20%:AX2, 20%:AX3, 30%, 30%:AX1, 30%:AX2, 30%:AX3, 40%, 40%:AX1, 40%:AX2, 40%:AX3, 55%, 55%:AX1, 55%:AX2, 55%:AX3, 70%, 70%:AX1, 70%:AX2, 70%:AX3, 80%, 80%:AX1, 80%:AX2, and 80%:AX3 are 186 kN, 193 kN, 198 kN, 202 kN, 202.5 kN, 206 kN, 211 kN, 214 kN, 216 kN, 220 kN, 224 kN, 228 kN, 231 kN, 234 kN, 238 kN, 242 kN, 244 kN, 247 kN, 250 kN, 253 kN, 254 kN, 255 kN, 256 kN, and 259 kN respectively. As shown in the Figure 4.1, the lowest lateral loading value of the parametric results would be from 20% (360 MPa) initial prestressing with 186 kN and the highest lateral loading value from 80%:AX3 (1440 MPa:1400 kN) initial prestressing with 259 kN

Referring to Figure 4.1, it clearly shown that with increasing initial prestressing from 20% to 80%, the lateral loading shows a significant increase of average 3 kN It can be said that the increase in initial prestressing contributes to the increase of overall stiffness of the column as the column does not have any reinforcement protruded through the column segments. The use of segments for the column adds horizontal shear that provide rigidity of the column structure. It can be seen that after the simulation is done, there will be an opening at the first segment, second segment and third segment of the column with the first segment have largest opening due to lateral displacement as shown in Figure 4.2(b).

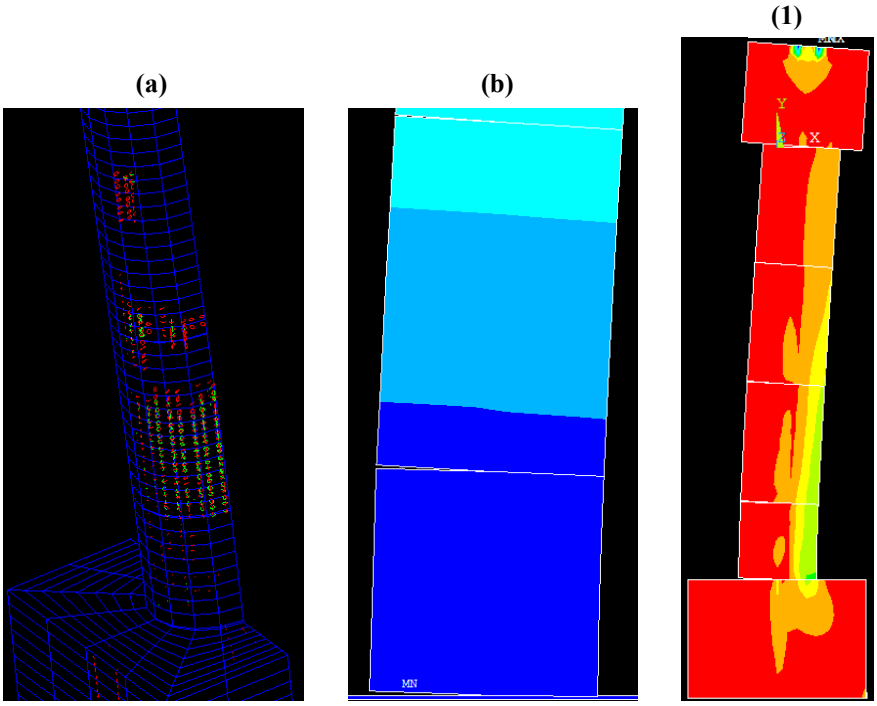

Figure 4.2: a) Cracks and crushing; b) Segments opening; c) Stress distribution of initial model of the initial model.

4.1.2 Axial Loading Parameter

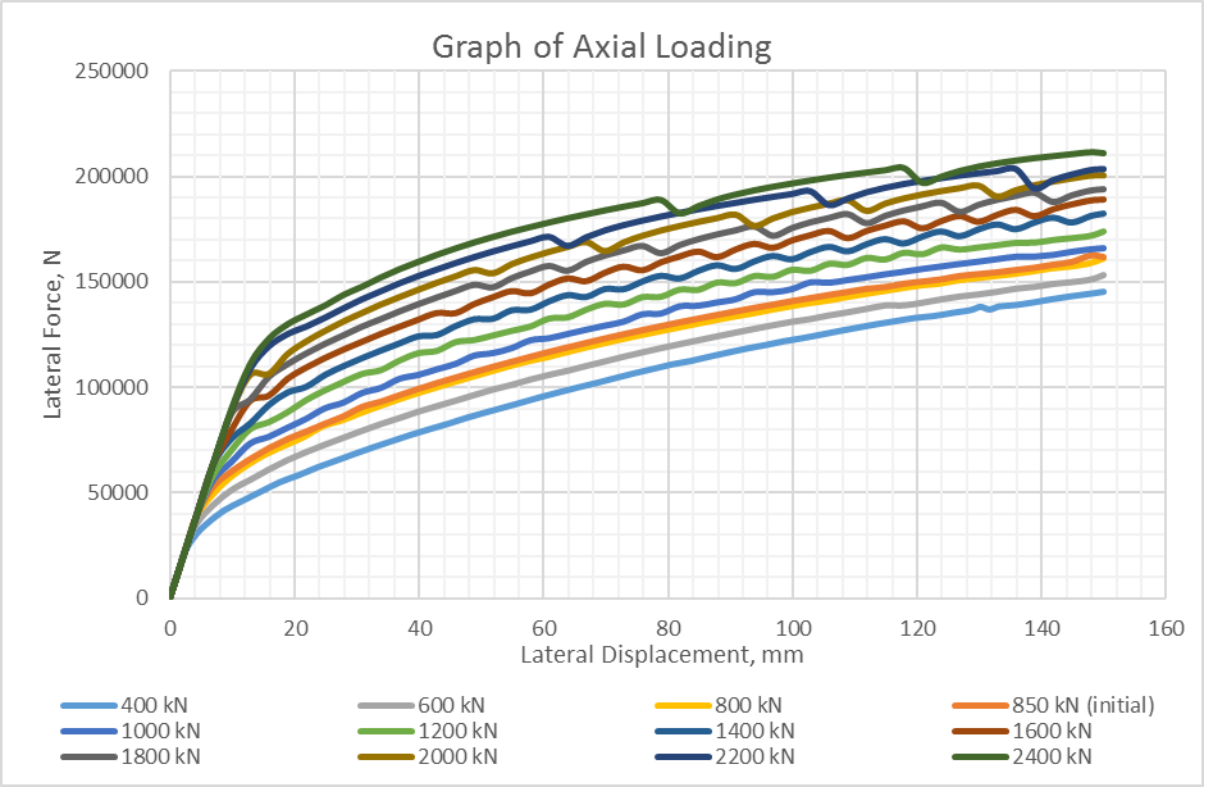

Figure 4.3: Graph of axial loading comparison.

Figure 4.3 shows the comparison of all 12 results for axial loading conditions. The axial loading conditions applied are 400 kN, 600 kN, 800 kN, 850 kN, 1000 kN, 1200 kN, 1400 kN, 1600 kN, 1800 kN, 2000 kN, 2200 kN, and 2400 kN The result from initial model of axial loading of 850 kN resulting in 162 kN of lateral loading. The results from parametric study on axial loading conditions resulting in 145 kN, 153 kN, 161 kN, 166 kN, 174 kN, 183 kN, 189 kN, 194 kN, 201 kN, 204 kN, and 211 kN of lateral loadings. The results acquired are taken from the precast segmental post-tensioned column undergone 150 mm lateral displacement simulation. As shown in Figure 4.3, the lowest lateral loading value of the parametric results would be from 400 kN axial loading with 145 kN and the highest lateral loading value from 2400 kN axial loading with 211 kN

Referring to Figure 4.3, it clearly shown that with increasing axial loading from 400 kN to 2400 kN, the lateral loading shows a significant increase of average 6.6 kN It can be

said that the application of axial loading downwards the column structure has reduced the moment acted on the column by lateral loading on the column head. That is why larger lateral loading is required to overcome the axial loading applied and also helps to increase the horizontal shear between segments.

4.1.3 Segments Parameter

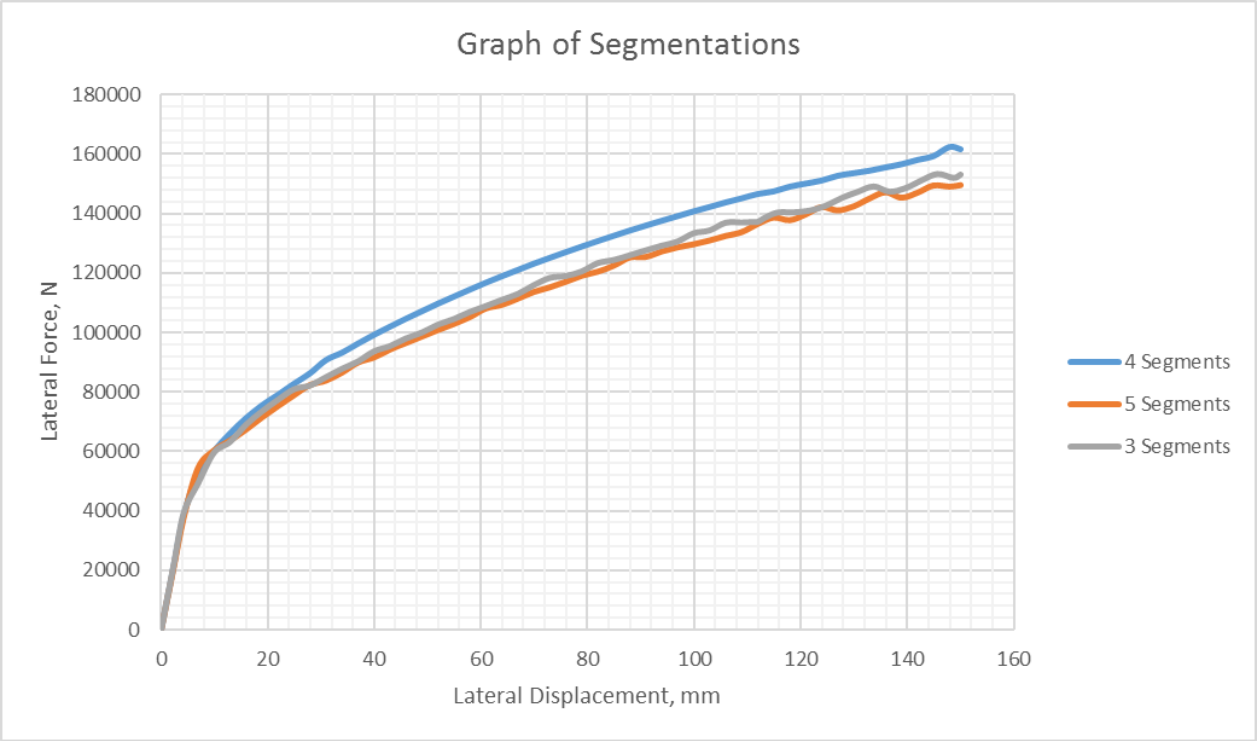

Figure 4.4: Graph of number of segments comparison.

Figure 4.4 shows the comparison of all 3 results for number of segments conditions. The number of segments conditions applied are 3 segments, 4 segments (initial model) and 5 segments. The result from initial model of 4 segments resulting in 162 kN of lateral loading. The results from parametric study on number of segments conditions resulting in 150 kN and 153 kN of lateral loadings. The results acquired are taken from the precast segmental post-tensioned column undergone 150 mm lateral displacement simulation. As shown in Figure 4.4, the lowest lateral loading value of the parametric results would be

from 3 segments with 150 kN and the highest lateral loading value from 4 segments with 162 kN

4.1.4 Concrete Strength Parameter

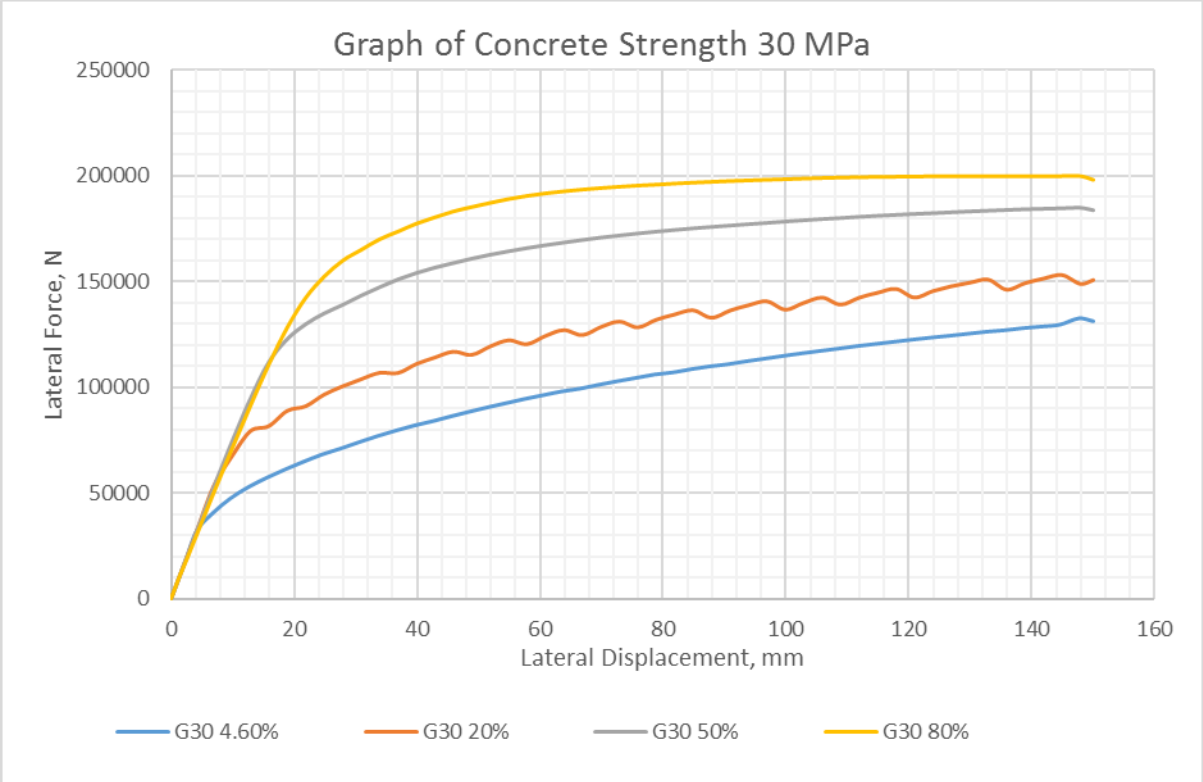

Figure 4.5: Graph of concrete strength 30 MPa comparison.

Figure 4.5 show the comparison of 4 column models of concrete strength 30 MPa. The additional condition applied is the variation of initial prestresses which are 4.6%, 20%, 50% and 80%. The results for concrete strength 30 MPa for initial prestresses 4.6%, 30% 50% and 80% are 131 kN, 151 kN, 184 kN and 198 kN respectively. The results show positive increase for the variations of initial prestresses. The observed result for G30 with 80% initial prestress shows the lateral force starts to be constant at 84.9 mm lateral displacement with 197 kN lateral force and the longest constant state at 117.9 mm lateral displacement with 200 kN lateral force. The lateral force drops to 198 kN at the end of simulation. This shows that the post-tensioning tendons have reached its elastic limit.

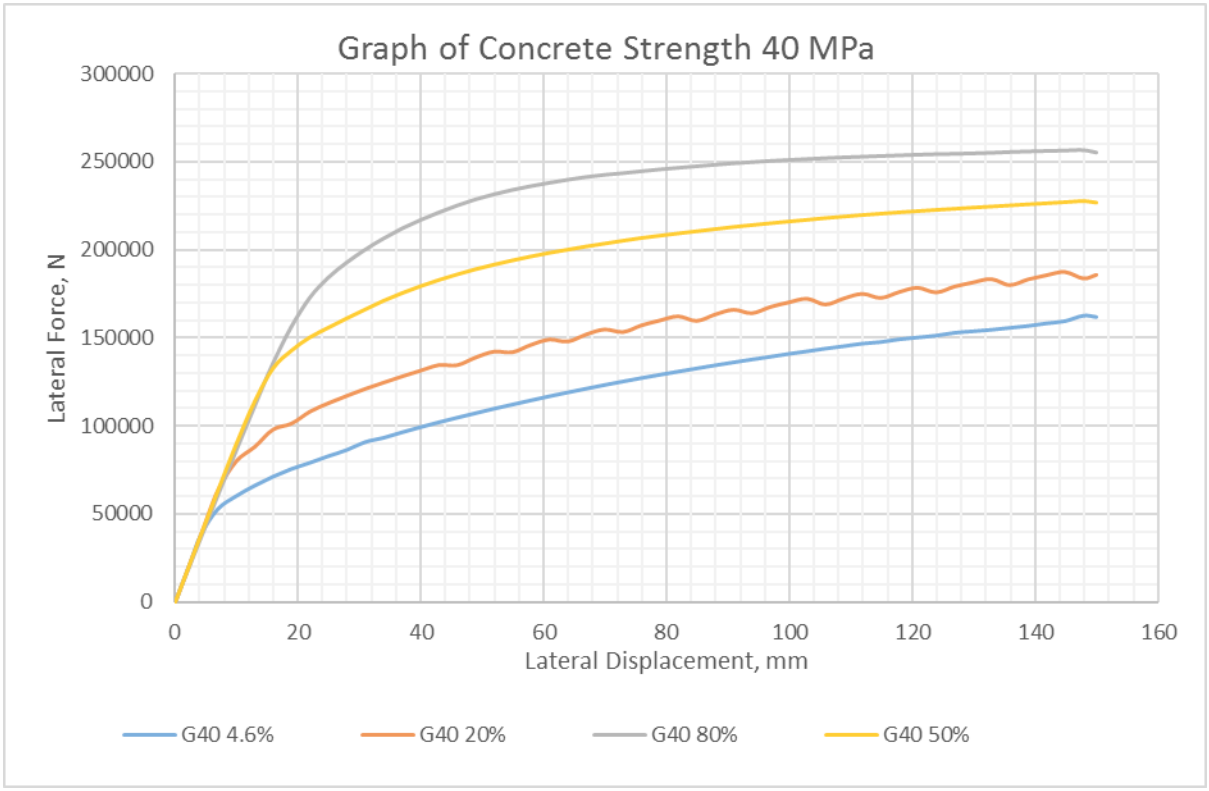

Figure 4.6: Graph of concrete strength 40 MPa comparison.

Figure 4.6 show the comparison of 4 column models of concrete strength 40 MPa. The additional condition applied is the variation of initial prestresses which are 4.6%, 20%, 50% and 80%. The results for concrete strength 40 MPa for initial prestresses 4.6%, 30% 50% and 80% are 162 kN, 186 kN, 227 kN, and 255 kN respectively. The results show positive increase for the variations of initial prestresses.

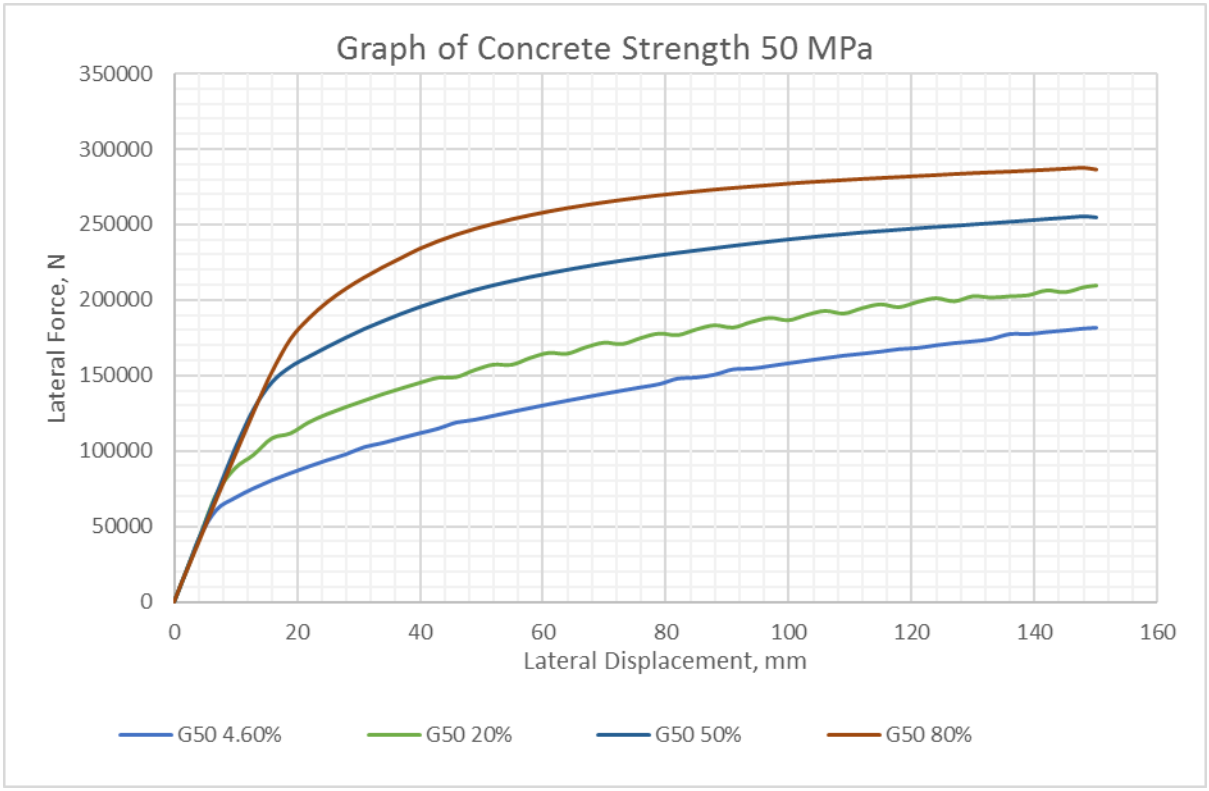

Figure 4.7: Graph of concrete strength 50 MPa comparison.

Figure 4.7 show the comparison of 4 column models of concrete strength 50 MPa. The additional condition applied is the variation of initial prestresses which are 4.6%, 20%, 50% and 80%. The results for concrete strength 50 MPa for initial prestresses 4.6%, 30% 50% and 80% are 182 kN, 210 kN, 255 kN, and 287 kN respectively. The results show positive increase for the variations of initial prestresses.

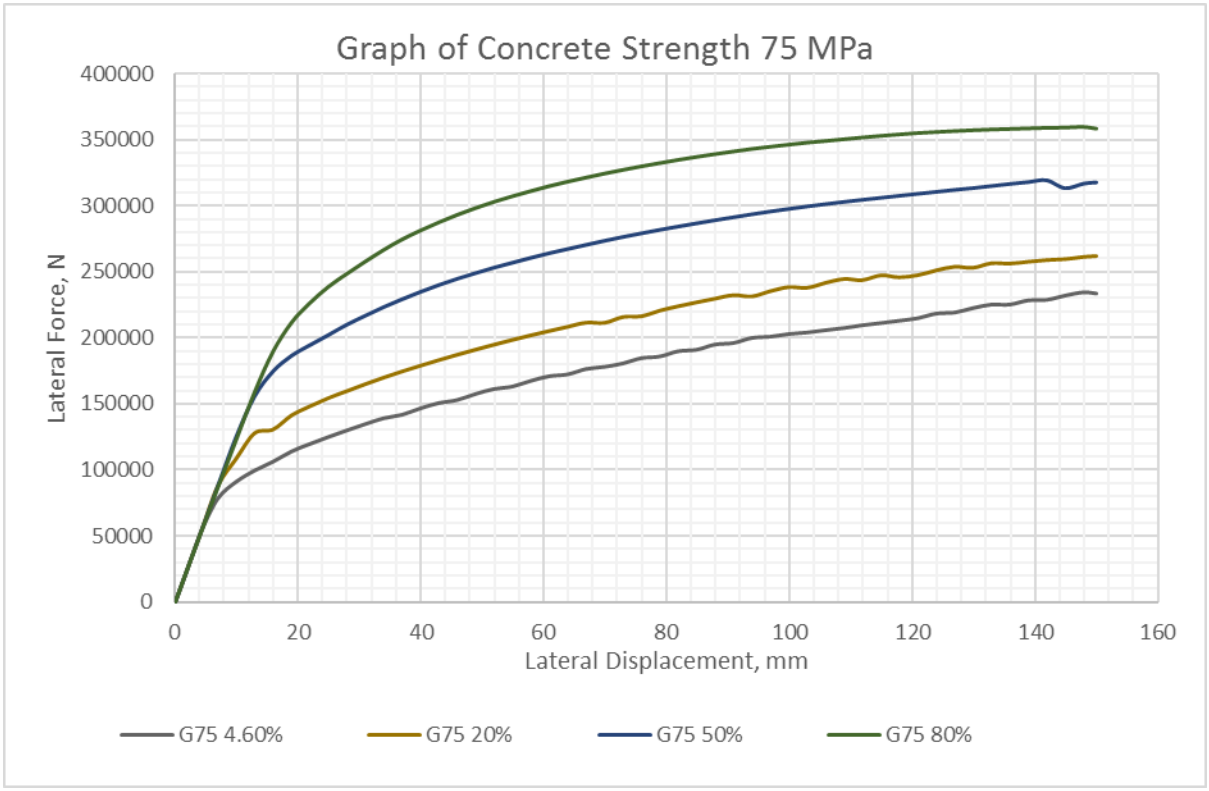

Figure 4.8: Graph of concrete strength 75 MPa comparison.

Figure 4.8 show the comparison of 4 column models of concrete strength 75 MPa. The additional condition applied is the variation of initial prestresses which are 4.6%, 20%, 50% and 80%. The results for concrete strength 75 MPa for initial prestresses 4.6%, 30% 50% and 80% are 234 kN, 262 kN, 318 kN, and 358 kN respectively. The results show positive increase for the variations of initial prestresses.

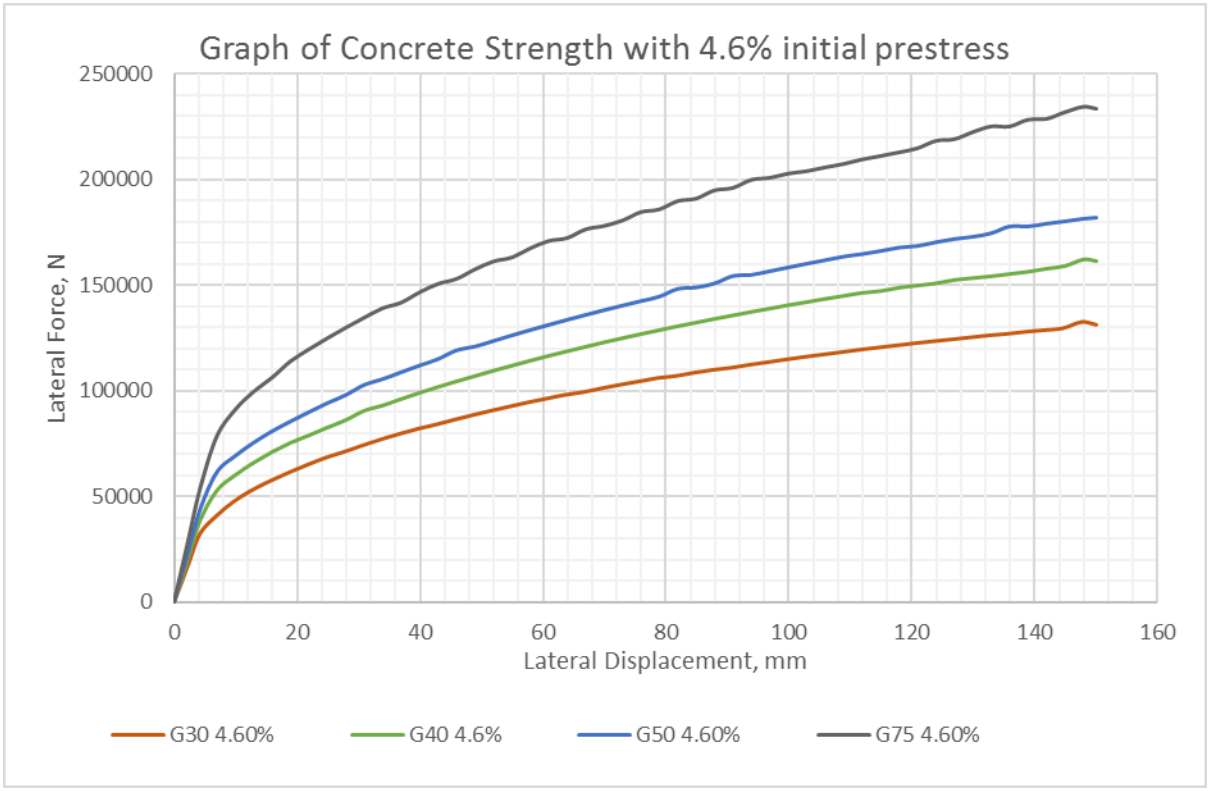

Figure 4.9: Graph of concrete strength with 4.6% initial prestress.

Figure 4.9 show the comparison of 4 column models of concrete strength 30 MPa, 40 MPa, 50 MPa and 75 MPa with 4.6% initial prestress. The results for concrete strength 30 MPa, 40 MPa, 50 MPa and 75 MPa are 131 kN, 162 kN, 182 kN, and 234 kN respectively. The results show positive increase for the variations of concrete strength.

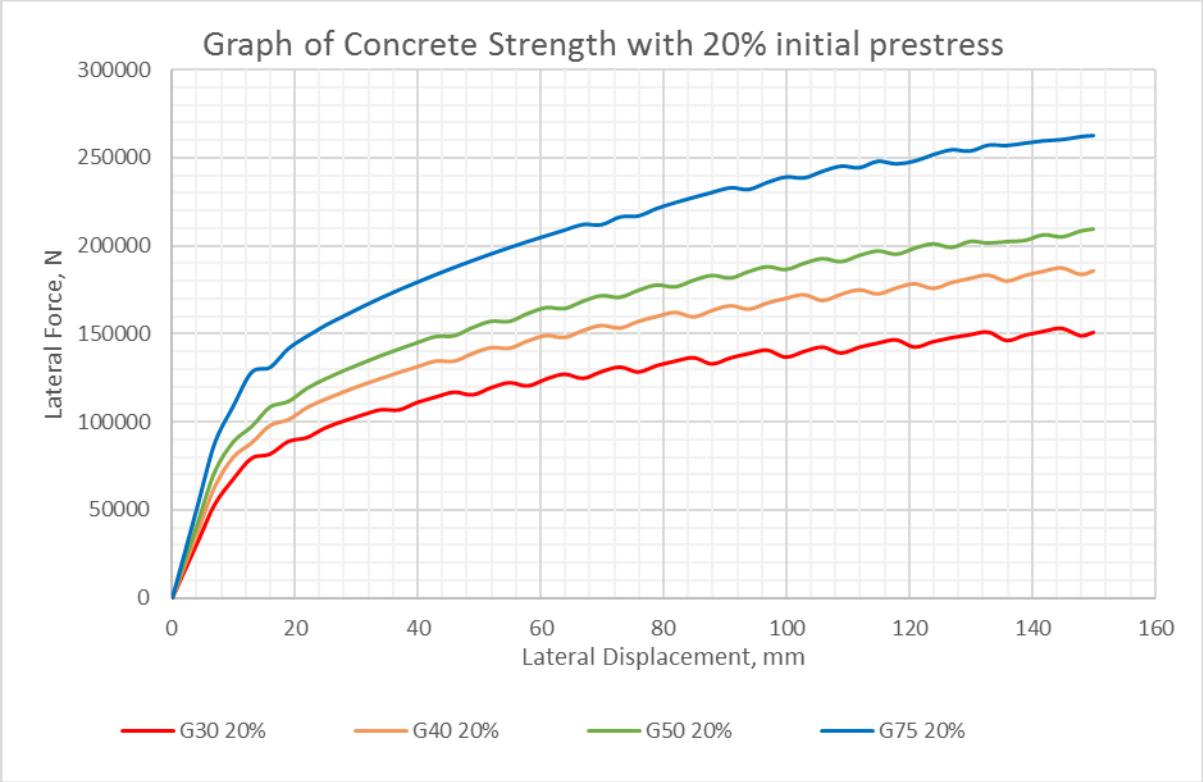

Figure 4.10: Graph of concrete strength with 20% initial prestress.

Figure 4.10 show the comparison of 4 column models of concrete strength 30 MPa, 40 MPa, 50 MPa and 75 MPa with 20% initial prestress. The results for concrete strength 30 MPa, 40 MPa, 50 MPa and 75 MPa are 151 kN, 186 kN, 210 kN, and 262 kN respectively. The results show positive increase for the variations of concrete strength.

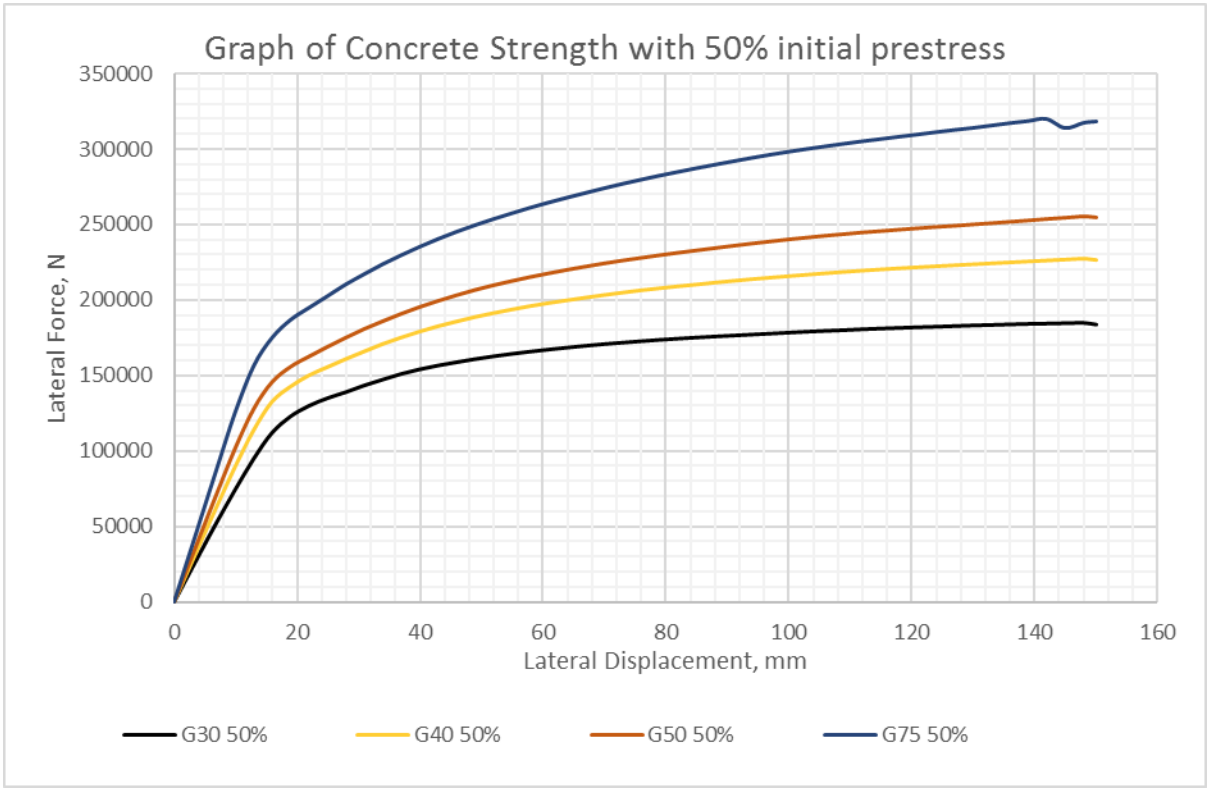

Figure 4.11: Graph of concrete strength with 50% initial prestress.

Figure 4.11 show the comparison of 4 column models of concrete strength 30 MPa, 40 MPa, 50 MPa and 75 MPa with 50% initial prestress. The results for concrete strength 30 MPa, 40 MPa, 50 MPa and 75 MPa are 184 kN, 227 kN, 255 kN, and 318 kN respectively. The results show positive increase for the variations of concrete strength.

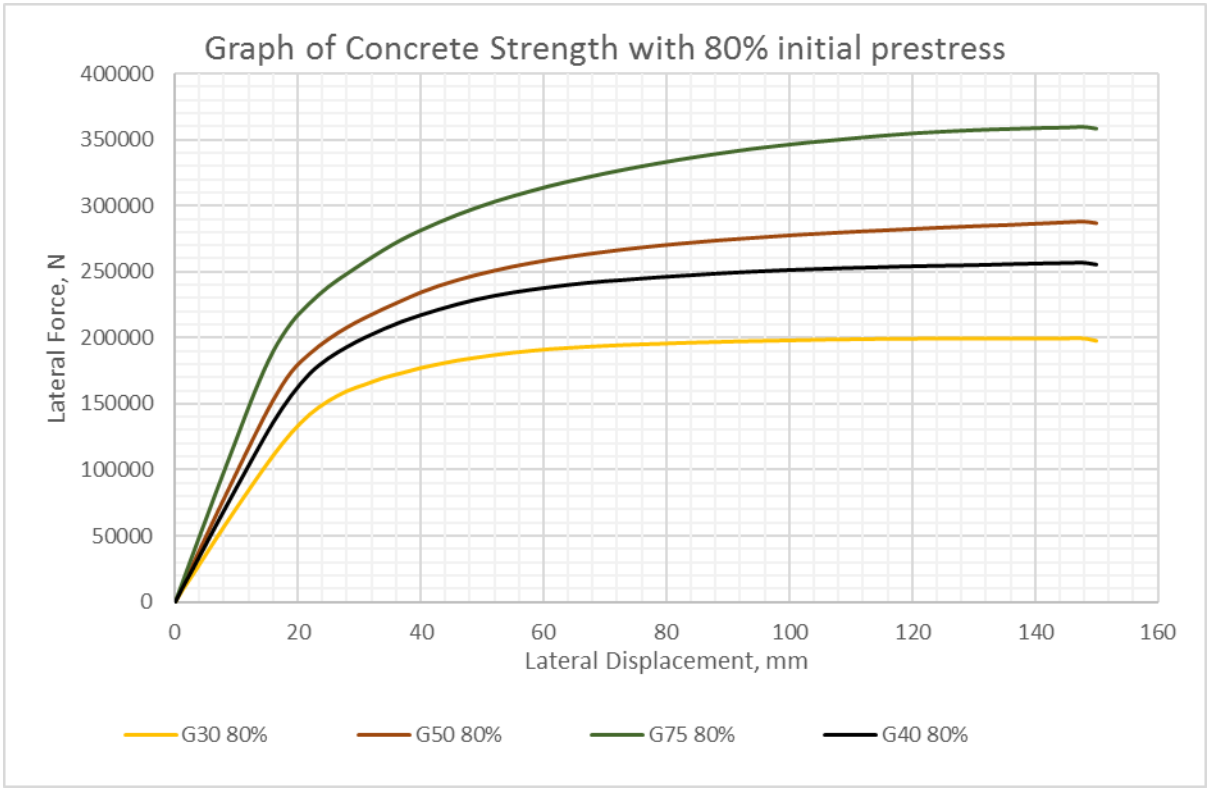

Figure 4.12: Graph of concrete strength with 80% initial prestress.

Figure 4.12 show the comparison of 4 column models of concrete strength 30 MPa, 40 MPa, 50 MPa and 75 MPa with 80% initial prestress. The results for concrete strength 30 MPa, 40 MPa, 50 MPa and 75 MPa are 198 kN, 255 kN, 287 kN, and 358 kN respectively. The results show positive increase for the variations of concrete strength.

4.1.5 Regression Study On Axial Loading and Initial Prestressing

In this project, regression analysis is made to analyse the relationship between studied variables. In this case, the relationship between alpha, α and maximum lateral loading are studied. The values of maximum lateral loading are acquired from the simulation results and while the values for alpha, α are calculated from the following equation:

$$Alpha, \alpha = \frac{P_g + P_p}{f'_c A_g}$$

Where P_g is the axial loading acted on the column structure,

P_p is the prestressing force that calculated from $P_p = \%\ initial\ strain \times \sigma_T \times A_g$

f'_c is the compressive strength of concrete, and

A_g is the cross-sectional area of the column.

All the data for regression study are tabulated as shown in Table 4.1 for axial loading, Table 4.2 for the initial prestressing and Table 4.3 for the combination between axial loading and initial prestressing.

Table 4.1: Data table for axial loading regression study.

Model	Axial per node	% initial strain	Pg	Pp	Fc'	Ag	α	Lateral Load
Axial 7	100000	4.6%	400000	220579.2	41.4	292246.66	0.05	145342.79
Axial 8	150000	4.6%	600000	220579.2	41.4	292246.66	0.07	153290.48
Axial 9	200000	4.6%	800000	220579.2	41.4	292246.66	0.08	161388.16
Axial 1	250000	4.6%	1000000	220579.2	41.4	292246.66	0.10	166180.91
Axial 2	300000	4.6%	1200000	220579.2	41.4	292246.66	0.12	173847.9
Axial 3	350000	4.6%	1400000	220579.2	41.4	292246.66	0.13	182624.13
Axial 4	400000	4.6%	1600000	220579.2	41.4	292246.66	0.15	189043.78
Axial 5	450000	4.6%	1800000	220579.2	41.4	292246.66	0.17	193679.74
Axial 6	500000	4.6%	2000000	220579.2	41.4	292246.66	0.18	200547.32
Axial 10	550000	4.6%	2200000	220579.2	41.4	292246.66	0.20	203821.44
Axial 11	600000	4.6%	2400000	220579.2	41.4	292246.66	0.22	211343.89

Note: The value for Pg is four times the value applied on node since the axial loading is applied on two nodes in the model and the model is symmetry.

Table 4.2: Data table for initial prestressing regression study.

Model	Axial per node	% initial strain	Pg	Pp	Fc'	Ag	α	Lateral Load
Prelim	211732.5	4.6%	846930	220579.2	41.4	292246.66	0.09	161604.9
PT 5	211732.5	20%	846930	959040	41.4	292246.66	0.15	185905.29
PT 5.1	250000	20%	1000000	959040	41.4	292246.66	0.16	193147.14
PT 5.2	300000	20%	1200000	959040	41.4	292246.66	0.18	198354.65
PT 6	211732.5	30%	846930	1438560	41.4	292246.66	0.19	202458.44
PT 5.3	350000	20%	1400000	959040	41.4	292246.66	0.19	201600.33
PT 6.1	250000	30%	1000000	1438560	41.4	292246.66	0.20	205728.14
PT 6.2	300000	30%	1200000	1438560	41.4	292246.66	0.22	211363.22
PT 1	211732.5	40%	846930	1918080	41.4	292246.66	0.23	216039.87
PT 6.3	350000	30%	1400000	1438560	41.4	292246.66	0.23	213869.20
PT 1.1	250000	40%	1000000	1918080	41.4	292246.66	0.24	219622.40
PT 1.2	300000	40%	1200000	1918080	41.4	292246.66	0.26	223705.56
PT 1.3	350000	40%	1400000	1918080	41.4	292246.66	0.27	228168.20
PT 2	211732.5	55%	846930	2637360	41.4	292246.66	0.29	231419.21
PT 2.1	250000	55%	1000000	2637360	41.4	292246.66	0.30	234456.41
PT 2.2	300000	55%	1200000	2637360	41.4	292246.66	0.32	238268.37
PT 2.3	350000	55%	1400000	2637360	41.4	292246.66	0.33	241622.10
PT 3	211732.5	70%	846930	3356640	41.4	292246.66	0.35	244328.7
PT 3.1	250000	70%	1000000	3356640	41.4	292246.66	0.36	246894.84
PT 3.2	300000	70%	1200000	3356640	41.4	292246.66	0.38	249967.33
PT 4	211732.5	80%	846930	3836160	41.4	292246.66	0.39	255115.64
PT 3.3	350000	70%	1400000	3356640	41.4	292246.66	0.39	252706.82
PT 4.1	250000	80%	1000000	3836160	41.4	292246.66	0.40	253994.19
PT 4.2	300000	80%	1200000	3836160	41.4	292246.66	0.42	256243.49
PT 4.3	350000	80%	1400000	3836160	41.4	292246.66	0.43	258767.26

Table 4.3: Data table for combination of axial loading and initial prestress regression study.

Model	Axial per node	% initial strain	Pg	Pp	Fc'	Ag	α	Lateral Load
Axial 7	100000	4.6%	400000	220579.2	41.4	292246.66	0.05	145342.79
Axial 8	150000	4.6%	600000	220579.2	41.4	292246.66	0.07	153290.48
Axial 9	200000	4.6%	800000	220579.2	41.4	292246.66	0.08	161388.16
Prelim	211732.5	4.6%	846930	220579.2	41.4	292246.66	0.09	161604.9
Axial 1	250000	4.6%	1000000	220579.2	41.4	292246.66	0.10	166180.91
Axial 2	300000	4.6%	1200000	220579.2	41.4	292246.66	0.12	173847.9
Axial 3	350000	4.6%	1400000	220579.2	41.4	292246.66	0.13	182624.13
PT 5	211732.5	20%	846930	959040	41.4	292246.66	0.15	185905.29
Axial 4	400000	4.6%	1600000	220579.2	41.4	292246.66	0.15	189043.78
PT 5.1	250000	20%	1000000	959040	41.4	292246.66	0.16	193147.14
Axial 5	450000	4.6%	1800000	220579.2	41.4	292246.66	0.17	193679.74
PT 5.2	300000	20%	1200000	959040	41.4	292246.66	0.18	198354.65
Axial 6	500000	4.6%	2000000	220579.2	41.4	292246.66	0.18	200547.32
PT 6	211732.5	30%	846930	1438560	41.4	292246.66	0.19	202458.44
PT 5.3	350000	20%	1400000	959040	41.4	292246.66	0.19	201600.33
Axial 10	550000	4.6%	2200000	220579.2	41.4	292246.66	0.20	203821.44
PT 6.1	250000	30%	1000000	1438560	41.4	292246.66	0.20	205728.14
Axial 11	600000	4.6%	2400000	220579.2	41.4	292246.66	0.22	211343.89
PT 6.2	300000	30%	1200000	1438560	41.4	292246.66	0.22	211363.22
PT 1	211732.5	40%	846930	1918080	41.4	292246.66	0.23	216039.87
PT 6.3	350000	30%	1400000	1438560	41.4	292246.66	0.23	213869.20
PT 1.1	250000	40%	1000000	1918080	41.4	292246.66	0.24	219622.40
PT 1.2	300000	40%	1200000	1918080	41.4	292246.66	0.26	223705.56
PT 1.3	350000	40%	1400000	1918080	41.4	292246.66	0.27	228168.20
PT 2	211732.5	55%	846930	2637360	41.4	292246.66	0.29	231419.21
PT 2.1	250000	55%	1000000	2637360	41.4	292246.66	0.30	234456.41
PT 2.2	300000	55%	1200000	2637360	41.4	292246.66	0.32	238268.37
PT 2.3	350000	55%	1400000	2637360	41.4	292246.66	0.33	241622.10
PT 3	211732.5	70%	846930	3356640	41.4	292246.66	0.35	244328.7
PT 3.1	250000	70%	1000000	3356640	41.4	292246.66	0.36	246894.84
PT 3.2	300000	70%	1200000	3356640	41.4	292246.66	0.38	249967.33
PT 4	211732.5	80%	846930	3836160	41.4	292246.66	0.39	255115.64
PT 3.3	350000	70%	1400000	3356640	41.4	292246.66	0.39	252706.82
PT 4.1	250000	80%	1000000	3836160	41.4	292246.66	0.40	253994.19
PT 4.2	300000	80%	1200000	3836160	41.4	292246.66	0.42	256243.49
PT 4.3	350000	80%	1400000	3836160	41.4	292246.66	0.43	258767.26

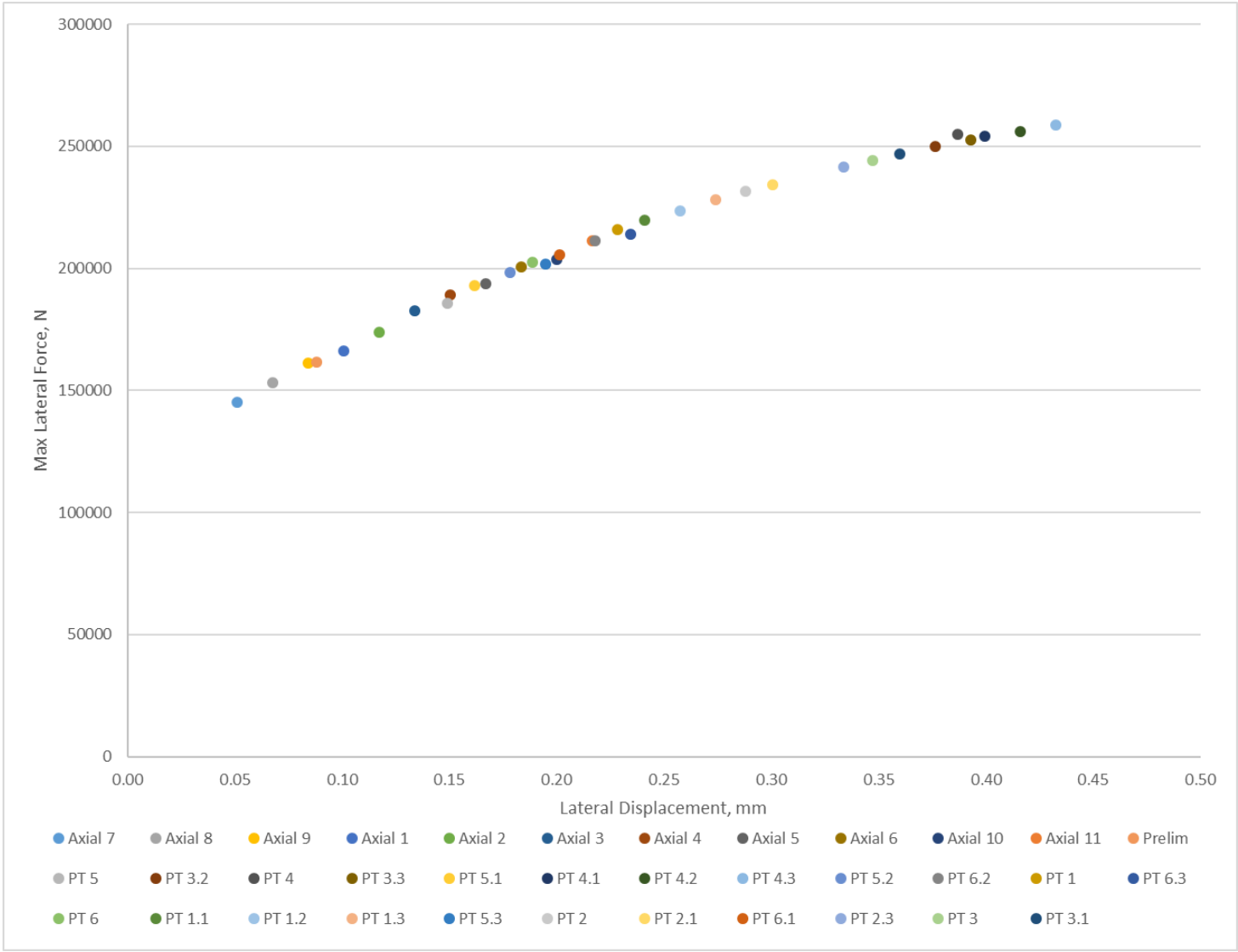

Figure 4.13: Scatter plot graph for both axial loading and initial prestress.

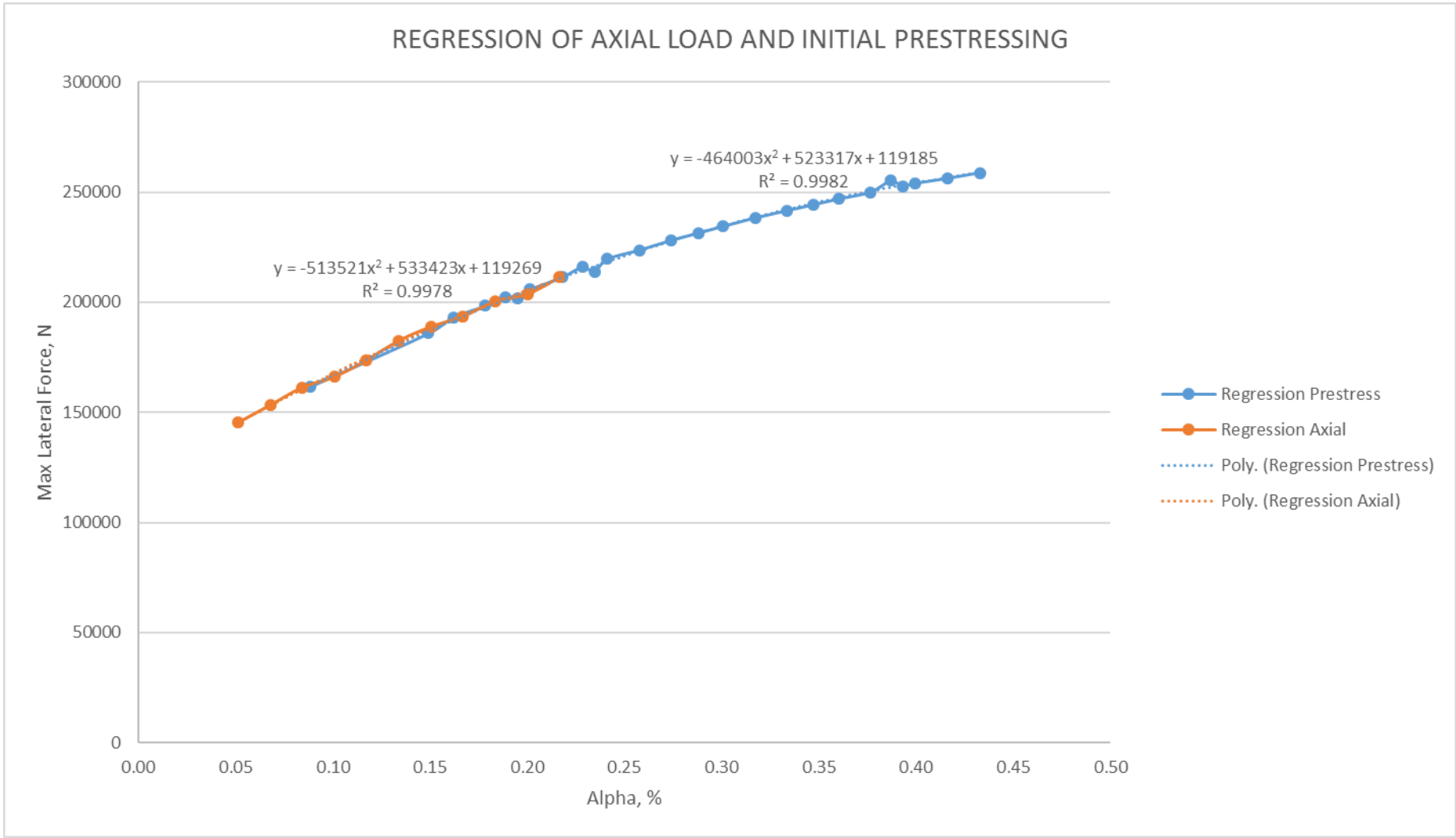

Figure 4.14: Regression graph plot for axial loading and initial prestress.

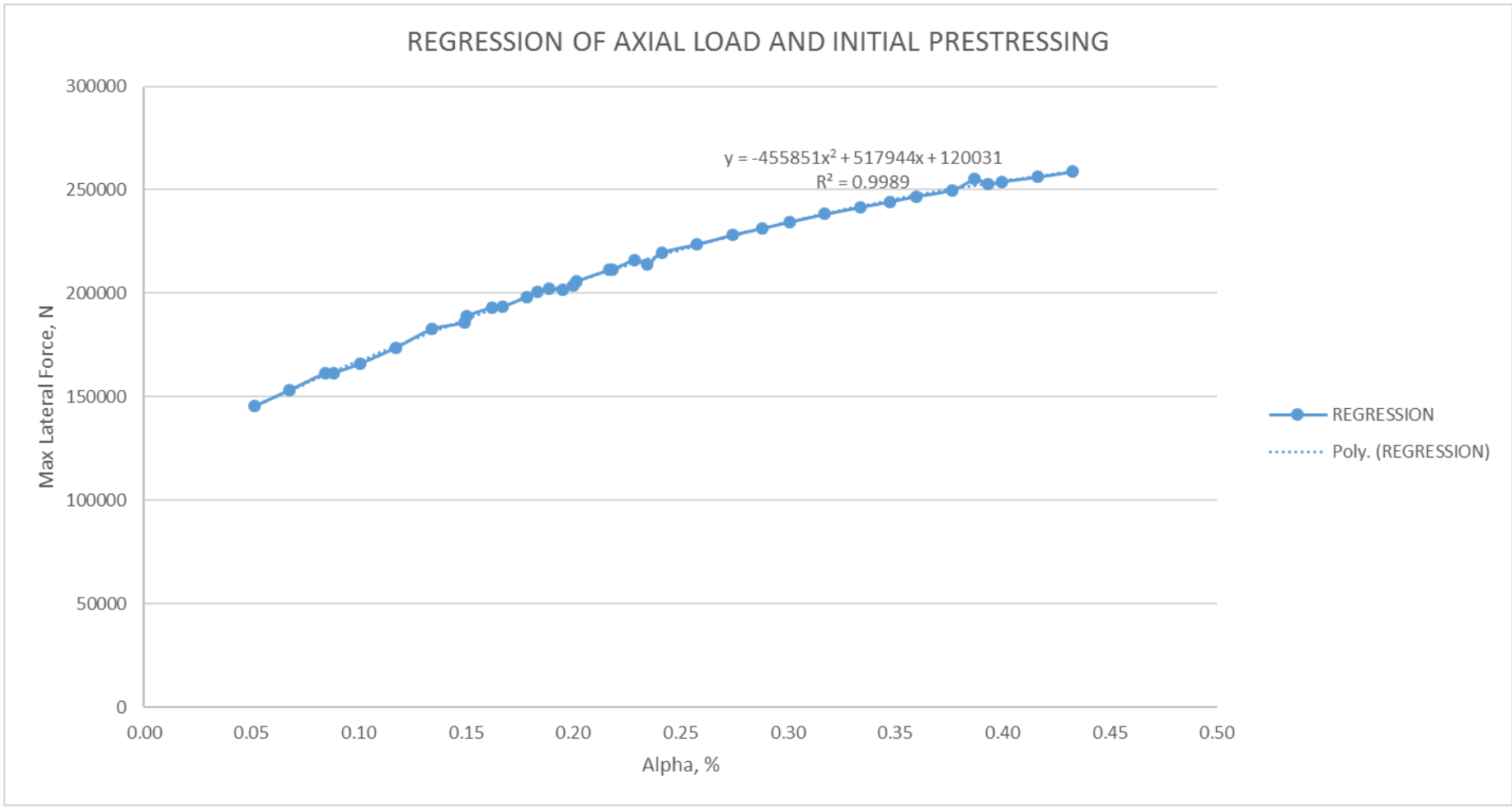

Figure 4.15: Regression graph plot for combination of both axial loading and initial prestress.

From Figure 4.14, the regression formula for both axial loading and initial prestress can be acquired. The equations are as follow:

For axial loading: $Max\ lateral\ force, F = -513521\alpha^2 + 533423\alpha + 119269$

For initial prestress: $Max\ lateral\ force, F = -464003\alpha^2 + 523317\alpha + 119185$

From Figure 4.15, the regression formula for the combination of axial loading and initial prestress can be acquired. The equation is as follow:

$$Max\ lateral\ force, F = -455851\alpha^2 + 517944\alpha + 120031$$

CHAPTER 5

CONCLUSION

Through this model simulations, the main design parameters that were investigated are initial prestressing, axial loading, column segments, and concrete strength and the condition for the simulation is the lateral displacement is set at 150 mm as to retain the functionality of the column itself and to find out the maximum lateral force it can sustain. Based on the methodology, the models were developed in stages and are done properly in a timely manner. Relating to this project objectives, all of the objectives has been achieved. The column models have been subjected to pushover analysis simulation and the performance for each models has been determined. Through this project, it is proven that axial loading has a significant effect on the lateral behaviour of the column in terms of lateral force. Based on the results from parametric studies, the highest maximum lateral force for initial prestressing, axial loading, column segments, and concrete strength are 258 kN, 211 kN, 161 kN, and 358 kN respectively. Further study need to be done to make a better comparison of the performance of each parameters that affecting the maximum lateral force. From this research, the performance of the column governs by the parameters studied could be used for forecasting the maximum lateral force from the regression formula.

REFERENCES

Billington, S.L., Barnes, R.W., and Breen, J.E. 2001. Alternate Substructure Systems for Standard Highway Bridges, J. Bridge Eng., 10.1061/(ASCE)1084-0702(2001)6:2(87), 87-94.

Shahawy, M.A. 2003. Prefabricated Bridge Elements and Systems to Limit Traffic Disruption During Construction, Technical Report, Transportation Research Board.

Chou, C.-C., Chang, H.-J., Hewes, J.T. 2013. Two-plastic-hinge and Two Dimensional Finite Element Models for Post-Tensioned Precast Concrete Segmental Bridge Columns, Engineering Structures, Volume 46, January 2013, 205-217.

Dawood, H., ElGawady, M., and Hewes, J. 2012. Behavior of Segmental Precast Posttensioned Bridge Piers under Lateral Loads., J. Bridge Eng., 10.1061/(ASCE)BE.1943-5592.0000252, 735-746.

Erkmen, B., and Schultz, A.E. 2007. Self-centering behaviour of unbonded precast concrete shear walls, Earthquake Resistance Engineering Structures VI, 185-194.

Hewes, J.T., and Priestley, M.J.N. 2002. Seismic Design and Performance of Precast Concrete Segmental Bridge Columns. Rep. No. SSRP-2001/25, University of California, San Diego.

Ou, Y., Chiewanichakorn, M., Aref, A., and Lee, G. 2007. Seismic Performance of Segmental Precast Unbonded Posttensioned Concrete Bridge Columns., J. Struct. Eng., 10.1061/(ASCE)0733-9445(2007)133:11(1636), 1636-1647.

Shim, C.S., Chung, C.-H., Kim, H.H. 2008. Experimental evaluation of seismic performance of precast segmental bridge piers with a circular solid section, Engineering Structures, Volume 30, Issue 12, December 2008, 3782-3792.

Zhang, X., Hao, H., Li, C. 2016. Experimental investigation of the response of precast segmental columns subjected to impact loading, International Journal of Impact Engineering, Volume 95, September 2016, 105-124.